République Algérienne Démocratique et Populaire
وزارة التعليم العالي والبحث العلمي
Ministère de l'Enseignement Supérieur et de la Recherche Scientifique

iversité – Mohamed El Bachir Ibrahimi Bordj Bou Arreridj
culté des Sciences et de la Technologie
partement Sciences de la Matière

جامعة محمد البشير الإبراهيمي « برج بوعريريج »
ية العلوم والتكنولوجيا
سم علوم المادة

UNIVERSITE MOHAMED EL BACHIR EL IBRAHIMI
BORDJ BOU ARRERIDJ

Mémoire de fin d'études

PRESENTÉ EN VUE DE L'OBTENTION
DU DIPLOME DE: Master

Filière :Physique
Option : Physique des Matériaux

THÈME :

Implémentation des conditions aux limites de la boite numérique pour la résolution de l'équation de Schrödinger dépendante du temps

Préparé par : **Saoudi Imene**

Soutenu le **:**--/--/2021

Devant le jury :

Président : N. Benchiheub	M.C.B. Université de BBA
Rapporteur: N. Grar	M.C.A Université de BBA
Examinateur : F. Khalfallah	M.C.A. Université de BBA

Année Universitaire 2020-2021

Remerciment

- je tiens avant tout à remercier le miséricordieux tout puissant, car sans son aide rien de cela n'aurait pu être possible
- A mes parents
- A mes chères sœurs, A mes chers frères, et à ma chère tante vos encouragements ont été ma motivation durant ce travail, c'est l'occasion pour moi de vous remercier très sincèrement. puisse votre présence m'inspirer à toujours aller de lavant
- J'exprime ma profonde gratitude et respectueuse reconnaissance a mon encadreur « *Dr N. Grar*» pour son suivi durant la préparation de ce mémoire de Master et pour les commentaires utiles.
- Je tien aussi a remercier tous les membres du jury qui m'ont fait l'honneur d'accepter de juger mon travail
- A tous mes amis qui ont toujours été à mes côtés dans les bons et les mauvais moments en particulier mes chères amies «*Imene* »

Abstract

Solving numerically the Schrodinger equation occupies an important place in quantum physic. However an enormous problem we are encountering when searching for such a solution is the limitation of the size of the numerical box. In this master thesis we are exploitiny the crank Nicolson method to solve the Schrodinger equation, then a comparative study is conducted between some methods devised to avoid numerical back reflexion at the boundaries of the numerical box

Résumé

Une solution numérique à l'équation de Schrödinger occupe une place importante en physique quantique. Cependant un énorme problème auquel on fait face quand on cherche à établir une telle solution est la limitation de la taille de la boite numérique. Dans ce mémoire de master on exploite la méthode de Crank Nicolson pour résoudre l'équation de Schrödinger, une étude comparative est conduite entre certaines méthodes établies pour éviter la réflexion numérique qui a lien aux limites de la boite numérique

ملخص

ان الحل الرقمي لمعادلة شرودينغر تحتل مكانة مهمة في الفيزياء الكم, غير ان مشكلة كبرى تواجهنا حين نبحث عن مثل هكذا حل وهو محدودية العلبة الرقمية, من خلال مذكرة الماستر هذه نستغل طريقة كرانك نكلسون في حل معاذلة شرودينغر وبعدها تقوم بدراسة مقارنة بين بعض الطرق المقترحة لتجنب الانعكاس الرقمي الذي يحدث عند حدود العلبة الرقمية

Content

figures List

Figures **Page**

Introduction

Quantum mechanics has proven to be a very powerful theoretical tool in investigating the microscopic world. Based on a set of postulates, this discipline never revealed to be wrong for nearly a century after its Birth. Among these postulates the most important one is unmistakably the Schrodinger equation. This is so because a solution to this differential equation is sufficient to provide all the information we need to describe any quantal system. Unfortunately analytical solutions for the Schrödinger equation are possible only for some theoretical or very simple physical cases (infinite well, square well, hydrogen atom…). For most of the cases of interest a numerical approach is unavoidable.

The Schrödinger equation can be treated according to the physical interest into two frameworks: the time independent and time dependent forms. It is straight forward to describe any system that evolves in time in the time dependent framework. However the time independent frame is not to be eliminated de facto as it is a frame that imposes the time evolution as stationary and is not completely time independent. It is then important to analyze facts that make one frame or the other more appropriate physically.

In order to resolve the Schrödinger equation numerically the literature proposes a large set of approaches each with its own advantages and inconvenient. The selection of any candidate among these approaches is subject to a set of criteria that encompasses the constraints of the physical problem but also the constraints related to the numerical implementation in addition to the restriction imposed by the resources of the used calculator.

The scope of this study is to address one of the numerical problems we are encountering when trying to resolve the time dependent Schrodinger equation. Namely we are dealing with the limitation of the size of the numerical box which is the numerical space used to discretize the equation. This limitation is a restriction due to the limitation of the calculator memory. In reality the wave function that we are targeting through the solution should evolve in the whole space. The main concern with this restriction is that we can have a back reflection at the boundaries of the box that can contaminate the derived observations especially for cases where the results at large distances are important. We can enlarge the box to the extent where the reflection becomes a very remote artifact but this induces more memory resources thing that we want to avoid.

In this master project we are reviewing the most important techniques that could be used to suppress the back reflection at the edges. Our aim through this investigation is to establish a comparison between advantages and inconvenient between these different

techniques. In order to proceed towards this goal we should first provide a tool that resolves numerically the time dependent Schrodinger equation. This is established through a program we coded in FORTRAN language that uses the Crank-Nicolson numerical model for solving the equation.

This master thesis is organized as follows:

-The first chapter is a brief recall of the theory behind the Schrodinger equation. It details also the physical need for the wave packet rather than a wave function for an appropriate description of the system state. It ends with an exposé of the different strategies used to solve the Schrodinger equation. A special emphasize is devoted to the Crank Nicolson method as it is the method we used in our coding.

-A second chapter is an overview of some of the most important methods used to overcome the concern of the back reflection. The aim of this chapter is to understand theory behind different methods that can allow us to argue about the established results during the implementation.

-In the last chapter we will present the coded program used for the time dependent Schrodinger equation solution. It will also address the implementation of the different suppression methods in this program. The different results will be compared in order to derive conclusive comments.

Chapter 1: The time evolution of a quantum Gaussian wave packet

I. Introduction

It is well known that the starting point for the study of any quantum system is the resolution of the Schrodinger equation. In fact the resolution permits finding the eigenstates and the eigenvalues that can allow the calculation of any physical quantity related to the system. The resolution can be performed either in a time dependent or time independent framework depending on the researched features of the system. Some introductory examples in quantum physics can be established analytically and can be a starting point to evaluate other more complicated situations.

In this first chapter we aim at presenting a simple method to solve the time-dependent Schrödinger equation by using a standard Crank–Nicholson method together with a Cayley's form for the finite-difference representation of evolution operator. Before doing this we introduce some basic concepts necessary to understand the theory of the Schrodinger equation.

II. The Schrödinger Equation

At the beginning of the 20th century, it had become clear that light has a wave-corpuscle duality, that is to say that it could manifest itself, depending on the circumstances, either as a particle, the photon, or as an electromagnetic wave. Louis de Broglie proposed to generalize this duality to all known particles, although this hypothesis had the paradoxical consequence that electrons should be able to produce interferences like light, which was later verified by experiment. By analogy with the photon, Louis de Broglie associated to each free particle of: energy **E** and momentum **p** a frequency**ν** and a wavelength **λ** [1].

In 1926 Schrödinger wrote the general equations that govern the particle in nonrelativistic motion in a field of potential energy: it is a differential equation of the wave function with partial linear and homogeneous drift of the first order in time (t) and the second order in position (x), comparable to the equation of motion of Newton of a material point in classical mechanics.

The Schrödinger equation has two 'forms', one in which time explicitly appears, and so describes how the wave function of a particle will evolve in time. In general, the wave function behaves like a wave, and so the equation is often referred to as the time dependent

Schrödinger wave equation. The other is the equation in which the time dependence has been 'removed' and hence is known as the time independent Schrödinger equation and is found to describe, amongst other things, what the allowed energies of the particle are. These are not two separate, independent equations – the time independent equation can be derived readily from the time dependent equation (except if the potential is time dependent, a development we will not be discussing here). In the following we will describe how the first, time dependent equation can be 'derived', and in then how the second follows from the first [2].

II.1 The Time Dependent Schrodinger Wave Equation

In the problem of the particle in an infinite potential well, it was observed that the wave function of a particle of fixed energy E could most naturally be written as a linear combination of wave functions of the form:

$$\psi(x,t) = \psi_0 e^{i(kx-\omega t)} \tag{1.1}$$

The wave vector k and the angular frequency ω are properties of the wave and are related to momentum and energy (particle properties) according to the postulate expressed by the relations

$$p = \hbar k \tag{1.2}$$

$$E = \hbar\omega \tag{1.3}$$

Then :

$$\psi(x,t) = \psi_0 e^{\frac{i}{\hbar}(px-Et)} \tag{1.4}$$

We note that by deriving the wave with respect to time, it comes then that:

$$\frac{\partial}{\partial t}\psi(x,t) = -\frac{i}{\hbar}\psi_0 E e^{\frac{i}{\hbar}(px-Et)} = -\frac{i}{\hbar}E\psi(x,t) \tag{1.5}$$

$$E\psi(x,t) = i\hbar\frac{\partial}{\partial t}\psi(x,t) \tag{1.6}$$

Then the energy operator is:

$$E = i\hbar\frac{\partial}{\partial t} \tag{1.7}$$

Similarly, for the gradient of this wave function, we have:

$$\vec{\nabla}\psi = \frac{i}{\hbar}\vec{p}\psi(x,t) \tag{1.8}$$

So

$$\vec{p}\psi(x,t) = -i\hbar\vec{\nabla}\psi(x,t) \tag{1.9}$$

Therefore

$$\vec{p} = -i\hbar\vec{\nabla} \tag{1.10}$$

P is the momentum operator.

For a free particle, according to classical mechanics, the mechanical energy is given by:

$$T = \frac{p^2}{2m} \tag{1.11}$$

This quantity appears in the Hamiltonian formulation for a free particle (v(x)=0) of classical mechanics. By applying the principle of correspondence between the classical and quantum values, for the energy and the momentum of equation we obtain:

$$\frac{-\hbar^2}{2m}\Delta\psi(x,t) = i\hbar\frac{\partial}{\partial t}\psi(x,t) \tag{1.12}$$

Where: $\Delta = \overrightarrow{\nabla^2}$ is the Laplacian.

The Hamiltonian operator of the system for a free particle is:

$$H = \frac{-\hbar^2}{2m}\Delta \tag{1.13}$$

Using this operator, to simplify the writing of the Schrödinger equation we obtain:

$$H\psi(x,t) = E\psi(x,t) \tag{1.14}$$

When the particle is immersed in a scalar potential independent of time (for example potential of a harmonic oscillator) according to classical mechanics, the total energy of the system is written as follows:

$$E = \frac{p^2}{2m} + V(x) \tag{1.15}$$

With this new energy value and from equation (1.12) and the operator p, the Schrödinger equation becomes:

$$i\hbar\frac{\partial}{\partial t}\psi(x,t) = \left(\frac{-\hbar^2}{2m}\Delta + V(x)\right)\psi(x,t) \tag{1.16}$$

The Hamiltonian operator of the system is the

$$H = \frac{-\hbar^2}{2m}\Delta + V(x) \tag{1.17}$$

By using this operator, we can simplify the writing of the Schrödinger equation:

$$i\hbar\frac{\partial}{\partial t}\psi(x,t) = H\psi(x,t) \tag{1.18}$$

II.2 The Time Independent Schrodinger Equation:

We do know what the wave function looks like for a free particle of energy E and for the particle in an infinitely deep potential well though we did not obtain that result by solving the Schrodinger equation. But in both cases, the time dependence entered into the wave function via a complex exponential factor $e^{[-iEt/\hbar]}$. This suggests that to'extract' this time dependence we guess a solution to the Schrodinger wave equation of the form

$$\psi(x,t) = \psi(x)e^{-iEt/\hbar} \tag{1.19}$$

The idea now is to see if this guess enables us to derive an equation for ψ(x), the spatial part of the wave function. If we substitute this trial solution into the Schrodinger wave equation, and make use of the meaning of partial derivatives, we get:

$$\frac{-\hbar^2}{2m}\frac{d^2\psi(x)}{dx^2}e^{iEt/\hbar} + V(x)\psi(x)e^{iEt/\hbar} = i\hbar(-iE/\hbar e^{iEt/\hbar}\psi(x)) = E\psi(x)e^{iEt/\hbar} \tag{1.20}$$

We now see that the factor$e^{[-iEt/\hbar]}$ cancels from both sides of the equation, giving us:

$$\frac{-\hbar^2}{2m}\frac{d^2\psi(x)}{dx^2} + V(x)\psi(x) = E\psi(x) \tag{1.21}$$

II.3. The wave function

The solutions of the Schrödinger equation of a quantum system are called the wave functions, they can be considered as a quantum postulate that describes the quantum state of a particle and contains all the information that we want to know about the system. The wave function $\psi(x,t)$must satisfy the following conditions:

- It must be continuous for x.

- The derivative $\frac{\partial\psi}{\partial t}$ must be continuous,

These constraints are applied under the condition of the limit on the solutions.

- It must be normalized. This implies that the wave function approaches zero as x approaches infinity that is:

$$\int \psi^* \psi d^3r = \int |\psi|^2 d^3r = 1 \tag{1.22}$$

With $|\psi(x,t)|^2$ is the probability density.

Since we have seen that the Schrödinger equation is a first order partial differential equation with respect to time and second order with respect to spatial coordinates, it is a difficult equation to solve for most quantum systems except for some particular simple case where analytical solution can be achieved.

II.4 The wave packet

To introduce quantum mechanics we always talk about a wave function as representing the particle state. From other side we do know that the Schrödinger equation solution for a free particle is a plane wave (a sine function) that extends in the whole space. This comes as a natural consequence of the Heinsberg indetermination principle. Indeed, assuming in this case that the momenta of the particle is precisely determined ($\Delta p=0$) implies that $\Delta x=\infty$). We say that the particle is delocalized. This comes as a counter sense since we know that the particle is somewhere. The only way to circumvent this problem is to allow some uncertainty on the momenta P (or equivalently the wave vector k), this means that we are superposing a number of sine functions that leads to the creation of the wave packet fig 1.1. Actually the wave packet is a way to reconcile the corpuscle and wave natures of the quantum particles [3].

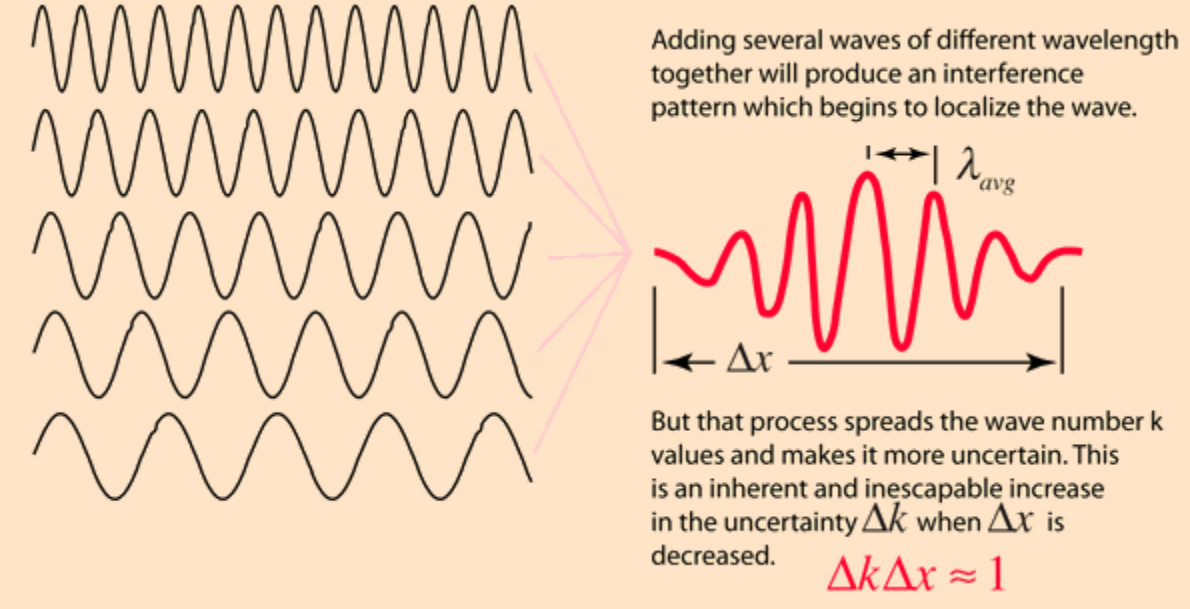

fig 1.1: Construction of a wave packet from sine function with different wave number k

A very well-known shape of the wave packet is a Gaussian form and can be given by the following mathematical expression:

$$\psi(x,t=0)=\left(\frac{1}{\sigma\sqrt{2\pi}}\right)^{1/2} exp\left[-\frac{1}{4}\left(\frac{x-x_0}{\sigma}\right)^2\right] \qquad (1.23)$$

Where σ is the variance and x_0 is the mean value. The coefficient of the exponent is normalizing this Gaussian (fig 1.2).

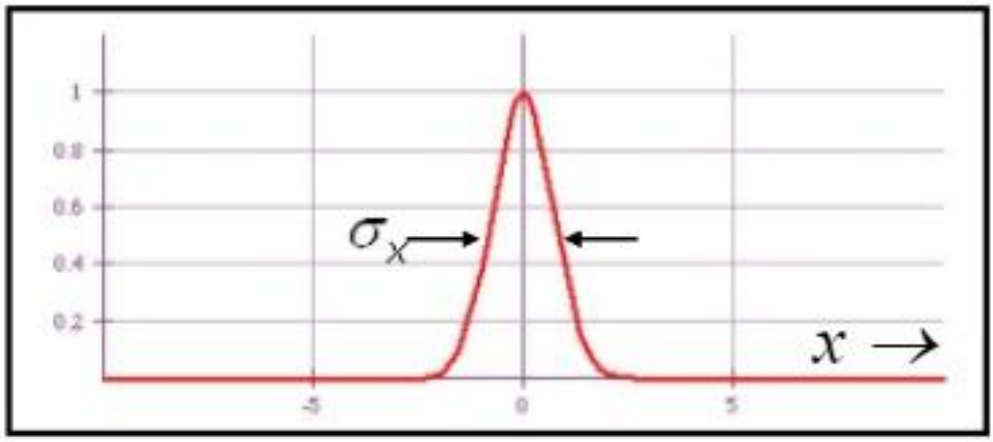

fig 1.2: A normalized Gaussian wave packet with a variance σ and centered around x_0=0

III. Evolution operator:

If we consider a time evolution of the wave function then the time become an explicit variable. Let us study the evolution of the wave function between an initial instant t_0 and an arbitrary instant *t*. In other words how $|\psi(t_0)\rangle$ becomes $|\psi(t)\rangle$. Because of the linear correspondence between $|\psi(t_0)\rangle$and $|\psi(t)\rangle$, there exists a unitary linear operator U(t,t_0), such that [4]:

$$|\psi(t)\rangle = U(t,t_0)|\psi(t_0)\rangle \tag{1.24}$$

It is clear, from the above formula that the role of this operator is to determine the evolution of the state at any time, for this reason it is called evolution operator. In the particularly simple case where the Hamiltonian H of the system does not depend on time, the operator U(t,t_0) has a simple form:

$$U(t,t_0) = e^{\frac{-i}{\hbar}H(t-t_0)} \tag{1.25}$$

Indeed, taking the partial derivative with respect to time of the function (1.25) we obtain:

$$i\hbar\frac{\partial}{\partial t}U(t,t_0) = HU(t,t_0) \tag{1.26}$$

We note that the equation (1.26) presents the same degree of difficulty as the Schrödinger equation, but it has more advantages when using the approximation methods. The total evolution operator can thus be decomposed into a product of operators of infinitesimal time evolution operators:

$$U(t,t_0) = U(t,t_k)U\left(t_k,t_{k_1}\right)\dots U(t_2,t_1)U(t_1,t_0) \tag{1.27}$$

We can choose $t_0, t_1 \dots t_k$ so that the intervals between them are equal. ThusU (t,t_0) can be written:

$$U(t,t_0)=\prod_{i=1}^{N}U_i(t_1,t_2-\Delta t) \tag{1.28}$$

We can conclude that the motion of a quantum ensemble can be assimilated toa succession of unitary transformations. A particular case of the transformation (1.24), having multiple applications in the diffusion theory of particles, is the one where the initial state is fixed not for t_0=0, but for $t_0=-\infty$ and the final state$|\psi(t)\rangle$ is considered for t = $+\infty$ then we have:

$$|\psi(+\infty)\rangle=U(-\infty,+\infty)|\psi(-\infty)\rangle \tag{1.29}$$

Where it is explicitly indicated that $t_0=-\infty$ the operator U being de defined by the formula

$$U=U(+\infty,-\infty)=\lim_{\substack{t\to+\infty\\ t_0\to-\infty}}U(t,t_0) \tag{1.30}$$

This operator is called the diffusion matrix.

IV. Solving the Time-Dependent Schrodinger Equation

Since we are interested in the time evolution of a Gaussian wave packet, it is straightforward to look for the ways to solve the time dependent Schrodinger equation. The solution for the time independent Schrodinger equation is however important to establish the profile of the solution for t_0 and then propagate this form for ulterior times. In our case this first step can be skipped, since we are assuming that the first solution is represented by a Gaussian wave packet, with well declared parameters. Consequently we will be only interested by the propagation phase and for this we should solve the time dependent Schrodinger equation. Let us first notice that there is two important points that we should feature in order to reach a compromise for the searched solution. The first point concerns the form adopted for the evolution operator and the second is rather numerical and concerns the formula adopted for the finite difference, representing the partial derivatives. In this section we examine both points. The aim is to be able to argue about the final choice we have adopted in our study.

Let us first recall the strategy of discretization for spatial and temporal derivative appearing in the Schrodinger equation.

IV.1 Spatial finite difference discretization

In the case of complicated potential fields V (x), the numerical finite difference is a method of choice, to solve the Schrodinger equation. For the time independent case we can simply discretize the space in the Schrodinger equation and put it into matrix form, which can

then be numerically solved. For the one dimensional case, the Schrodinger equation at each point along x can be written as [5]:

$$E\psi_{x_n} = -\frac{\hbar^2}{2m}\left(\frac{d^2\psi}{dx^2}\right)_{x_n} + V_n(x)\psi_{x_n} \tag{1.31}$$

Using the basic finite difference approximation

$$\left(\frac{d^2\psi}{dx^2}\right)_{x_n} = \frac{\psi_{x_{n+1}} - 2\psi_{x_n} + \psi_{x_{n-1}}}{\Delta x^2} \tag{1.32}$$

Where Δx is an uniform interval spacing, we can write equation (1.31) as:

$$\mathrm{E}\psi_{x_n} = K\left(2\psi_{x_n} - \psi_{x_{n+1}} - \psi_{x_{n-1}}\right) + V_n(x)\psi_{x_n} \tag{1.33}$$

With

$$\mathrm{K} = \frac{\hbar^2}{2m\Delta x^2} \tag{1.34}$$

This can also be written in matrix form as:

$$E\begin{pmatrix} \psi_1 \\ \psi_2 \\ \psi_3 \\ \vdots \\ \psi_{N-1} \\ \psi_N \end{pmatrix} = \begin{pmatrix} 2K+V_1 & -K & 0 & 0 & 0 & \cdots \\ -K & 2K+V_2 & -K & 0 & 0 & \cdots \\ 0 & -K & 2K+V_3 & -K & 0 & \cdots \\ \vdots & \vdots & & \ddots & \ddots & \vdots \\ \cdots & 0 & 0 & -K & 2K+V_{N-1} & -K \\ \cdots & 0 & 0 & 0 & -K & 2K+V_N \end{pmatrix}\begin{pmatrix} \psi_1 \\ \psi_2 \\ \psi_3 \\ \vdots \\ \psi_{N-1} \\ \psi_N \end{pmatrix} \tag{1.35}$$

This can also be written in operator form as:

$$EI\psi = H\psi \tag{1.36}$$

Where I is the identity matrix. This eigenvalue problem can be solved numerically, and the corresponding eigenvectors can be found.

IV.2 Temporal finite element discretization

Now we have to add to the temporal discretization to fully express the Schrodinger equation. This can be represented by the schematic of figure 1.3.

For the temporal derivative, we can have different methods to express the descritezation of the time dependent Schrodinger equation: forward Euler, backward Euler and fourth order Runge-Kutta [6].

• Forward Euler method consists in approximating the temporal derivative by:

$$\frac{\partial\psi(x,t)}{\partial t} \simeq \frac{\psi(x,t+\Delta t) - \psi(x,t)}{\Delta t} \tag{1.37}$$

The spatial part of the equation is given by:

$$H(x,t)[\psi(x,t)] \tag{1.38}$$

This method, despite being cheap in terms of computation, is relatively bad in terms of stability.

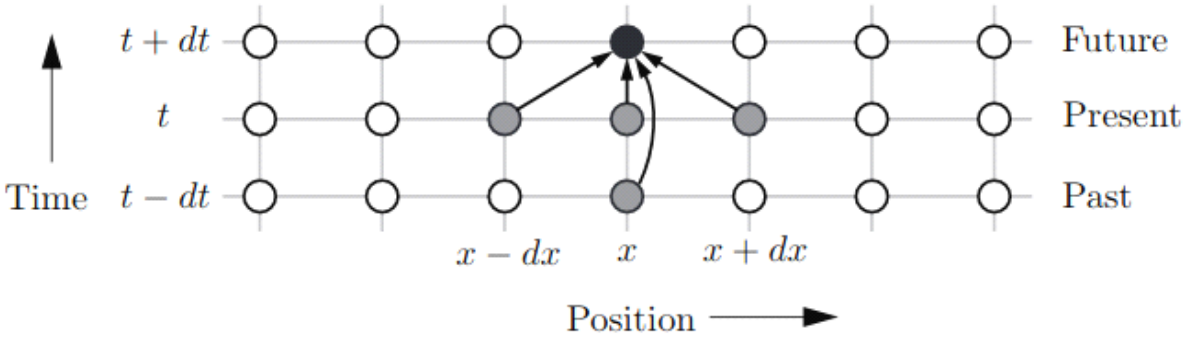

fig 1.3: Schematic representation of time and space descritization

• Backward Euler method is a modification to forward Euler that grants more stability at the cost of more computations per iteration. The temporal derivative is approximated as in forward Euler but now the spatial part is given by:

$$H(x,t)[\psi(x,t+\Delta t)] \tag{1.39}$$

so we need to solve an equation system each time step.

• Runge-Kutta of fourth order is a more complex explicit method based on quadratures that requires more computations every step, but has better convergence and stability.

Based mainly on the two first strategy of discretization, there are three different schemes of resolving the Schrödinger equation: Explicit scheme, implicit scheme and Crank-Nicolson scheme. Explicit methods calculate the state of a system at a later time from the state of the system at the current time, while an Implicit method finds it by solving an equation involving both the current state of the system and the later one. The Crank-Nicolson scheme is a special case of implicit scheme.

IV.3 Explicit method

Applying the explicit time-difference approximation for the time difference we have:

$$\left[\frac{d\psi(x,t)}{dt}\right]_{t=t_j,x=x_n} = \frac{\psi_{x_n}^{t_{j+1}} - \psi_{x_n}^{t_j}}{\Delta t} \tag{1.40}$$

A stable and unitary discretization is obtained by applying a centered time difference which leads to a three-step explicit method

$$\psi(i;n+1) = \psi(i;n-1) + i2\Delta t\left(\frac{\hbar}{2m}\frac{\psi(i-1;n) - 2\psi(i;n) + \psi(i+1;n)}{\Delta x^2} - \frac{V(i)}{\hbar}\psi(i;n)\right) \tag{1.41}$$

In operator form this can be written:

$$\psi^{t_{j+1}} = \left(I - \frac{i}{\hbar}\Delta t.H\right)\psi^{t_j} \tag{1.42}$$

Where as before H is the discretized Hamiltonian (with the potential matrix V) and I is the unit matrix. With, The explicit scheme is not always numerically stable, actually the condition under which explicit scheme is stable is:

$$0 < \left|\frac{k\hbar}{2m\Delta x^2}\right| < \frac{1}{2} \tag{1.43}$$

This is non unitary scheme because:$\left(I - \frac{i}{\hbar}\Delta tH\right)^* \left(I - \frac{i}{\hbar}\Delta tH\right) = I + \frac{\Delta t^2}{\hbar^2}H^2$, the operator $I - \frac{i}{\hbar}\Delta tH$ is not unitary which is the condition under which the probability is conserved.

IV.4 Implicit method

In Implicit Scheme, the state of a system at later time is calculated by solving a equation involving states both at current time and later time. Now performing an implicit discretization we have:

$$\psi_{x_n}^{t_j} = \psi_{x_n}^{t_{j+1}} + \frac{i}{\hbar}\Delta t\left[-\frac{\hbar^2}{2m\Delta x^2}\left(\psi_{x_{n+1}}^{t_{j+1}} - 2\psi_{x_n}^{t_{j+1}} + \psi_{x_{n-1}}^{t_{j+1}}\right) + V_{x_n}\psi_{x_n}^{t_{j+1}}\right] \tag{1.44}$$

which can also be put into operator form as:

$$\psi^{t_{j+1}} = \left(I + \frac{i}{\hbar}\Delta tH\right)^{-1}\psi^{t_j} \tag{1.45}$$

The fully implicit scheme is unconditionally stable. Similarly we can show this scheme do not correspond to a unitary transformation.

IV.5 Crank Nicolson method

The Crank Nicolson scheme is based on central difference in space, and the trapezoidal rule in time, giving second order convergence in time. Equivalently, it is the average of the Euler forward method and the Euler backward method in time. This leads to the following equation:

$$\begin{aligned} i\hbar\frac{\psi_n^{j+1} - \psi_n^j}{\Delta t} = \frac{1}{2}\left[-\frac{\hbar^2}{2m}\frac{d^2\psi(x,t)}{dx^2} + V(x)\psi(x,t)\right]_n^{j+1} \\ + \frac{1}{2}\left[-\frac{\hbar^2}{2m}\frac{d^2\psi(x,t)}{dx^2} + V(x)\psi(x,t)\right]_n^{j} \end{aligned} \tag{1.46}$$

After the spatial discretization this become:

$$i\hbar\frac{\psi_n^{j+1}-\psi_n^j}{\Delta t}=\frac{1}{2}\left[-\frac{\hbar^2}{2m\Delta x^2}\left(\psi_{x_{n+1}}^{t_{j+1}}-2\psi_{x_n}^{t_{j+1}}+\psi_{x_{n-1}}^{t_{j+1}}\right)+V_{x_n}\psi_{x_n}^{t_{j+1}}\right] + \frac{1}{2}\left[-\frac{\hbar^2}{2m\Delta x^2}\left(\psi_{x_{n+1}}^{t_j}-2\psi_{x_n}^{t_j}+\psi_{x_{n-1}}^{t_j}\right)+V_{x_n}\psi_{x_n}^{t_j}\right] \quad (1.47)$$

After rearranging terms the equation can be put in formal expression as:

$$(I+iH)\psi^{j+1}=(I-iH)\psi^j \quad (1.48)$$

Where H has now a modified form and is a tridiagonal matrix. We will explicit this in the coming section. So we have the numerical difference equation in the Cayley or the Crank Nicolson form:

$$\psi^{t_{j+1}}=\frac{I-iH}{I+iH}\psi^{t_j} \quad (1.49)$$

The temporal operator that relate ψ_j to ψ_{j+1} is now not only numerically stable but also unitary; this can be shown as:

$$\left(\frac{I-iH}{I+iH}\right)^*\left(\frac{I-iH}{I+iH}\right)=\left(\frac{I+iH}{I-iH}\right)\left(\frac{I-iH}{I+iH}\right)=I \quad (1.50)$$

Through this unitary property, equation (1.50) then satisfies conservation of probability as required.

From the analysis above, it follows that, numerical solutions of the time dependent Schrödinger discretized with finite differences can be accomplished using the explicit scheme or the Crank Nicholson implicit scheme. The explicit approach requires more memory storage, since the solution at three time levels must always be known. The implicit scheme requires the solution of a tridiagonal matrix at each time step.

V. choices for our study

After considering the most important thing to bear in mind when tackling the resolution of the time dependent Schrodinger equation, we opted for the use of the Crank Nicholson method in our coding. This is the case since the method is numerically stable and is acceptable in term of time consumption. We are presenting in this section the details of a simple method to solve the time-dependent Schrodinger equation by using a standard Crank Nicholson method together with a Cayley's form for the finite-difference representation of evolution operator as implemented in our program [7].

Let us consider the Schrodinger equation in atomic units, i.e. m = ħ = 1

$$i\frac{\partial}{\partial t}\psi(x,t)=H(x,t)\psi(x,t) \quad (1.51)$$

with the Hamiltonian given by

$$H(x,t) = \frac{-1}{2}\frac{\partial^2}{\partial x^2} + V(x,t) \tag{1.52}$$

The idea is to compute the time evolution of the wave function ψ (x, t) for $t > t_0$, given an initial state$\psi(x,t_0)$. We start by dividing the time interval into n subintervals of equal length $\Delta t = (t - t_0)/n$, and use an implicit Crank Nicholson integrator to propagate the wave function from one time step to the next one.

The formal solution to (1.51) could be expressed in terms of the time evolution operator as

$$\psi(x,t) = e^{(-iHt)}\psi(x,0) \tag{1.53}$$

The effective time evolution operator U for one discrete time step Δt, can be expressed using Cayley's form for the finite-difference representation of e^{-iHt}, whichis a combination of a fully implicit and a fully explicit method

$$U(t+\Delta t,t) = \frac{1-(i\Delta t/2)H(x,t)}{1+(i\Delta t/2)H(x,t)} \tag{1.54}$$

Such a representation of U is second-order accurate in space and time and also unitary. The integration scheme for the wave function then reads

$$\left(1+\frac{i\Delta t}{2}H(x,t)\right)\psi(x,t+\Delta t) = \left(1-\frac{i\Delta t}{2}H(x,t)\right)\psi(x,t) \tag{1.55}$$

The wave function can be expanded on a discrete lattice as

$$\psi(x,t_n) = \sum_{j=1}^{N}\psi_j^n X_j \tag{1.56}$$

Where $\psi_j^n = \psi(x_j,t_n)$ is the value of the wave function at the position x_j of the *j*th lattice site at time $t_n = t_0 + n\Delta t$ with a grid basis:

$$x_j = \begin{cases} 1, & x_j - \frac{1}{2}\Delta x \le x \le x_j + \frac{1}{2}\Delta x \\ 0, & otherwise \end{cases} \tag{1.57}$$

Here $\Delta x = (x_{max} - x_{min})/N$, with x_{max} and x_{min} the boundaries of the finite grid. Using the finite-difference representation for the kinetic part of the Hamiltonian, we have

$$\left(i \pm \frac{i\Delta t}{2}H\right)\psi(x_j,t_n) \simeq \psi_j^n \pm \frac{i\Delta t}{2}\left(-\frac{\psi_{j+1}^n - 2\psi_j^n + \psi_{j-1}^n}{2\Delta x^2} + V_j^n\psi_j^n\right) \tag{1.58}$$

With $V_n = V(x_j,t_n)$. By introducing $\psi^n = (\psi_1^n,\ldots,\psi_j^n,\ldots,\psi_N^n)$, the lattice representation of equation (1.55) finally reads

$$\psi^{n+1} = D_2^{-1}D_1\psi^n \tag{1.59}$$

Where we define

$$D_1 = \left(1 - \frac{i\Delta t}{2}H\right) = (1 - S)\,, \quad D_2 = \left(1 + \frac{i\Delta t}{2}H\right) = (1 + S) \tag{1.60}$$

With $S = (i\Delta t/2)H$. The matrix product can be rewritten as

$$D_2^{-1}D_{1=}(1 - S)^{-1}(1 + S) = 2D_2^{-1} - 1 \tag{1.61}$$

Then, the wave packet evolution is achieved just by inverting the matrix D_2.For the case of time-independent potentials, the explicit N × N representation of D_1 and D_2 reads

$$D_{1=}\begin{pmatrix} \gamma_1 & \alpha & & & & \\ \alpha & \gamma_2 & \alpha & & & \\ & \alpha & \gamma_3 & \alpha & & \\ & & \ddots & \ddots & \ddots & \\ & & & \alpha & \gamma_{N-1} & \alpha \\ & & & & \alpha & \gamma_N \end{pmatrix} \tag{1.62}$$

$$D_{2=}\begin{pmatrix} \xi_1 & -\alpha & & & & \\ -\alpha & \xi_2 & -\alpha & & & \\ & -\alpha & \xi_3 & -\alpha & & \\ & & \ddots & \ddots & \ddots & \\ & & & -\alpha & \xi_{N-1} & -\alpha \\ & & & & -\alpha & \xi_N \end{pmatrix} \tag{1.63}$$

With:

$$\alpha = \frac{i\Delta t}{4\Delta x^2}, \qquad \gamma_j = 1 - \beta_j, \qquad \xi_j = 1 + \beta_J, \quad and \;\; \beta_j = \frac{i\Delta t}{2}\left(\frac{1}{\Delta x^2} + V_j\right) \tag{1.64}$$

These are the basic ingredients that should be introduced in our program to establish the numerical solution for the time dependent Schrodinger equation.

Chapter 2: Methods for suppression of the numerical reflection

I. Introduction

The first chapter was dedicated to a review of some fundamentals related to the Schrodinger equation as well as the numerical aspects that could be exploited to resolve this equation in cases where analytical solutions are no longer possible. The aim was to understand the structure of the problem to be able to make a choice of a solution which is a compromise between simplicity, stability and memory resources. We have opted for a solution using the Cranck Nicolson method with the Cayley form of finite difference. In the solution proposed, the only task of importance to be elaborated is the inversion of the matrix D_1, which can be achieved easily by exploiting functionalities of programs in the Lapack library. The program established this way, can solve the Schrodinger equation with any linear form of the potential.

The problem that emerges when a numerical solution is searched is the fact that computational area must be limited to a finite grid because of the finite capacity of the computer memory. We talk generally about the limited size of the numerical box fig 2.1. This finite grid produces unwanted reflections at the artificial boundaries of the computational area. This reflection can be a source of error in many applications where the shape of wave packet at large distance is important in the interpretation of the simulation results, as it is the case for experiments with strong laser beams and high harmonic spectra [8]. To suppress this numerical artifact we should create mathematical conditions at the boundaries that simulate the motion of the wave packet as it should be the case in infinite space. In this chapter we will review an ensemble of methods that minimize this numerical artificial effect and suppress the back-reflection. Some of these methods will be implemented in our program and their performances will be evaluated in the next chapter.

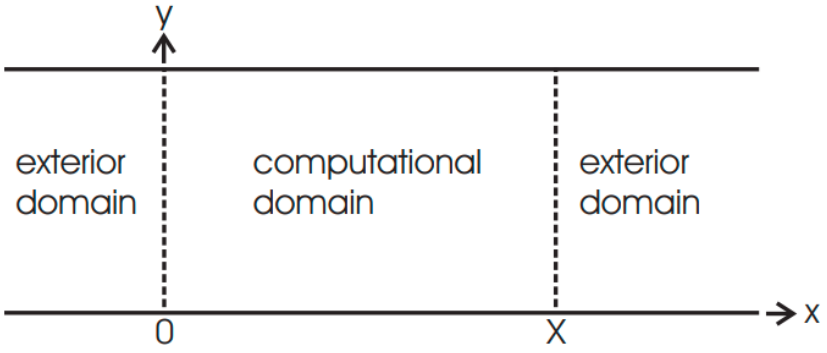

fig 2.1: Schematic of the artificial boundaries of the numerical box

II.The mask function

One of the simplest methods to eliminate the artificial reflection of wave packets is what we call masking functions. In this method a relaxation operator can be constructed and applied to the wave packet at the edge of the numerical box. Let M(r) be a masking function so that [9]:

$$M(r) = \begin{cases} 1 & if\, r < r_n \\ f(r) < 1 & if\, r_{N+1} \le r \le r_M \end{cases} \quad (2.1)$$

The range of lattice sites $r_{N+1}, \ldots, r_M$close to the reflecting wall now represent a finite subspace that corresponds to a finite number of lattice sites beyond the subspace $(r < r_n)$.In the region of the edge the wave function is allowed to relax by way of an amplitude-absorbing mask. The masking function f (r) can be chosen to be continuously differentiable at r_N to high order in order to minimize effects of discontinuities. Masking is effected by simply multiplying the state vector after every time interval Δt_j by the masking operator M which is diagonal in the lattice basis.The application of M is equivalent to a nonunitary evolution operator

$$U^M = exp(lnM) = exp\left(-iV_{opt}\Delta t\right) \quad (2.2)$$

generated by an optical potential V_{opt}

$$V_{opt} = i\,(lnM)/\Delta t \quad (2.3)$$

We note that masking functions introduce a specific classof optical potentials which can be expressed in terms of equation (2.3). However, an arbitrary smooth optical potential cannot, in general, be reduced to a simple masking function equation (2.1). U^Mdoes not explicitly depend on Δt.Implicitly, however, Δt enters through the application of themasking operator after every time interval Δt. A bunch of functions are proposed in the literature and only tests on several parameters of the problem can guide us throw the compromised choices one can do.

III. The complex absorbing potential

In order to avoid affection of the undesirable spurious reflections at the boundaries in the long time period, in a modern time-dependent wave packet calculation, usually a complex absorbing potential (CAP) of the form $V(x) = -iW(x)$ or an equivalent damping function is introduced near the edge of the grid to attenuate the wave function gradually . Due to its simplicity and local nature, the CAP gains general applications and usually is efficient. The method is effected by adding a complex potential $-iW(x)$ to the operator on the right hand side of the Schrodinger equation:

$$i\hbar\frac{\partial\Psi(x,t)}{\partial t} = -\frac{\hbar^2}{2m}\frac{\partial^2\Psi(x,t)}{\partial x^2} + V(x)\Psi(x,t) - iW(x)\Psi(x,t) \tag{2.4}$$

$W(x)$is typically zero everywhere, except near the numerical boundarywhere energy is absorbed by letting the real part of $W(x)$be positive. Much effort has been devoted to finding effective and optimized CAPs for different applications, by minimizing the reflection and the transmission coefficients [10]. The reflection and transmission coefficients describe the relation between the amplitudes of an incident wave and the waves that are reflected on and transmitted through the CAP, respectively. By minimizing the sum of the two the absorption is maximized. However, the reflection of the CAP increases with increasing frequency, while the transmission is reduced with increasing frequency. Thus, a CAP can only be optimized for certain frequencies. Also, numerical reflections arise from the region where the CAP is active, and pollute the solution in the interior.

When the distribution of the translational energy in the wave packet is of broad range, especially involving ultra-slow translational energy, the CAP becomes very inefficient. Since it must be strong enough to damp the part moving rapidly, at the same time, it must go up gently enough to avoid the reflection of the part moving slowly.The major advantage of the CAP is its simplicity. The major disadvantage is that it has required a relatively large spatial range to be effective, thus consuming non negligible computational resources.

Let us investigate how a CAP changes the norm [11]. This can be done by differentiating the norm as:

$$\begin{aligned}\frac{d}{dt}\|\psi^2\| = \frac{d}{dt}\langle\psi|\psi\rangle = \langle\dot{\psi}|\psi\rangle + \langle\psi|\dot{\psi}\rangle \quad &= \langle -iH\psi|\psi\rangle + \langle\psi|-iH\psi\rangle \\ &= i\langle\psi|H^+ - H|\psi\rangle\end{aligned} \tag{2.5}$$

With

$$\begin{aligned} H &= H_0 - i\eta W \qquad H_0 = H_0^+ \\ H^+ &= H_0 + i\eta W \qquad W = W^+ \quad (W \text{ being scalar}) \end{aligned} \tag{2.6}$$

Where η is a parameter controlling the strength of the potential.

It follows that:

$$\begin{aligned}\frac{d}{dt}\|\psi\|^2 &= -2\eta\langle\psi|W|\psi\rangle \\ \frac{d}{dt}\|\psi\| &= -\eta\frac{\langle\psi|W|\psi\rangle}{\|\psi\|}\end{aligned} \tag{2.7}$$

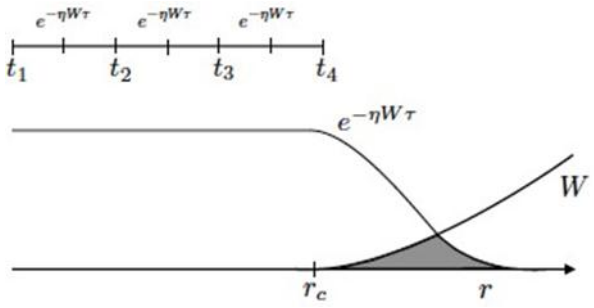

fig 2.2: Decrease of the norm of a wave packet being annihilated by a complex absorbing potential starting at r_c.

Hence the norm of the WF decreases when the wave packet enters the CAP. We want to inspect in more detail how the CAP annihilates the wave packet. We know the formal solution of the Schrödinger equation

$$\begin{aligned}\psi(t+\tau) &= e^{(-iH_0-\eta W)\tau}\psi(t) \\ &= e^{-iH_0\frac{\tau}{2}}e^{-\eta W\tau}e^{-iH_0\frac{\tau}{2}}\psi(t) + O(r^3)\end{aligned} \tag{2.8}$$

I.e. in the middle of each time step, the wave function is multiplied by $e^{-\eta W\tau}$ see fig 2.2. A correct location of the potential and the adequate range can ensure enough attenuation before reaching the edge and hence avoiding reflection fig 2.3

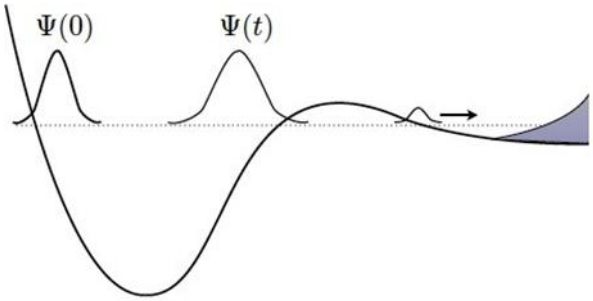

fig 2.3: Example of the correct location of a CAP.

The origin of the reflection is easy to understand. It is related to the Heisenberg uncertainty principle. We change the form of the wave packet, i.e. its coordinate distribution. But this implies that one also changes the momentum distribution which is just the Fourier-transform of the coordinate representation and this means reflection. To see this, let us turn to the time-independent picture fig 2.4:

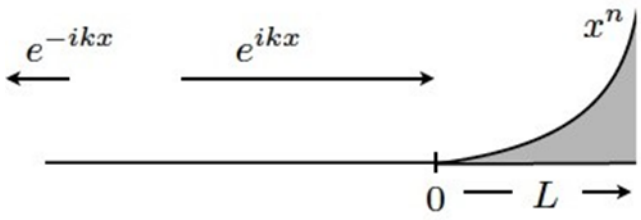

***fig 2.4**:* Illustration of CAP behavior in the time independent domain.

At energy *E* the wave function must be a linear combination of e^{ikx} and e^{-ikx} where the energy $E = k^2/2m$. Hence:

$$\psi(t) \sim e^{ikx} - Re^{-ikx} \text{ for } \quad x < 0 \tag{2.9}$$

Where R denotes the reflection coefficient. If we put an infinite wall at x = 0, we have total reflection (R = 1)

$$\psi(t) \sim e^{ikx} - e^{-kx} \sim sinkx \qquad \psi(0) \equiv 0 \tag{2.10}$$

Using scattering theory and semi classical arguments one can derive approximate formulas:

$$R^2 = \left|\frac{n!}{2^{n+2}}\right|^2 . \frac{\eta^2}{E^2 . k^2} = \left|\frac{n!}{2^{n+2}}\right|^2 . \left(\frac{\hbar^2}{2m}\right)^2 . \frac{\eta^2}{E^{n+2}} \tag{2.11}$$

$$T^2 = exp\left(-\frac{\eta L^{n+1} . 2m}{k(n+1)}\right) = exp\left(-\frac{\eta W(L)}{E} . \frac{k . L}{n+1}\right) \tag{2.12}$$

Where n is the number of time iteration where the attenuation is effective and L is the range of the CAP

One wants $T^2 + R^2 \ll 1$ this requires weak (η small) and long range (L large) CAPs. Note that k. L= 2π is equivalent to say that L equals one Debroglie wave length. A CAP should be at least two de-Broglie wavelengths long.

IV. The complex scaling of space coordinate

A more elegant and mathematically rigorous approach for dealing with the continuum is complex scaling of the spatial coordinate. Complex scaling involves an analytical continuation into the complex plane:

$$x \to xe^{i\theta} \tag{2.13}$$

Where θ is a positive and real constant. We can show that the resulting complex scaled Hamiltonian, $H_\theta(x) = H\left(xe^{i\theta}\right)$, has complex eigenvalues that are identified as resonances. The method of complex scaling provides a mean of dealing with both bound states and resonance states through the same formalism [12], since the eigenfunctions of H_θ are square-integrable. Although most frequently used in time-independent settings, this method was recently used for the time-dependent Schrodinger equation. The scaling of the Hamiltonian through (2.13) implies scaling of a

potential energy surface. This might be difficult, for instance if the potential is given as a set of abinitio points instead of an analytic expression. Exterior complex scaling (ECS) circumvents this issue to a large extent, by introducing the rotation into the complex plane beyond some $x = x_0$, where the potential is close to constant. For instance, if the potential is given as a set of points in the interaction region, but analytically continued in the asymptotic region, it is possible to perform the coordinate transformation for the potential for $x \geq x_0$. McCurdy et al. [13] recommend ECS for practical use of complex scaling in time-dependent problems. A similar approach to ECS is smooth exterior scaling (SES). The difference between ECS and SES consists of the transition to the complex plane being simply rotated or rotated through a smooth transition function. In the continuous setting, the SES interface is non-reflecting, whereas the ECS interface is not. From a numerical point of view, the smoothness of the transition function is of importance in order to avoid numerical reflections from the absorbing layer.

V. Transparent Boundary Conditions (CTBC)

The role of the absorbing boundary conditions is to eliminate the numerical reflection of the wave packet at the boundary of the numerical box , these are local boundary conditions that approximate the one way wave equation of a wave function. In this section we are going to expose the method by which we establish analytical solutions that can simulates a transparent boundaries. Since we deduce first the continuous solution and then discretize the result to introduce it in the numerical resolution, this strategy is known as transparent boundary condition (TBC) or coutinuous boundary condition (CTBC).

We have the Schrodinger equation depending on the time as:

$$i\hbar \frac{\partial}{\partial t}\psi(x,t) = \left(\frac{-\hbar^2}{2m}\frac{\partial^2}{\partial x^2} + V(x,t)\right)\psi(x,t) \tag{2.14}$$

In order to obtain the formulas for the absorbing boundary conditions, we consider the special solutions

$$\psi(x,t) = e^{(-i(\omega t - kx))} \tag{2.15}$$

These are states of definite energy E satisfying the dispersion relation

$$\hbar k = \mp\sqrt{2m(\hbar\omega - V)} \tag{2.16}$$

The absorbing boundary conditions must be designed to satisfy the dispersion relation given by the plus signed equation (2.16) at the boundary $x_{max}$and the minus signed at the boundary x_{min}. However, function (2.16) is not rational and cannot be converted into a partial differential equation, nonetheless, this relation can be linearly approximated by:

$$\hbar k = g_1(\hbar\omega - V) + g_2 \tag{2.17}$$

With :

$$g_1 = \mp\frac{\sqrt{2m\alpha_2} - \sqrt{2m\alpha_1}}{\alpha_2 - \alpha_1}, \quad g_2 = \mp\frac{\alpha_2\sqrt{2m\alpha_1} - \alpha_1\sqrt{2m\alpha_2}}{\alpha_2 - \alpha_1} \tag{2.18}$$

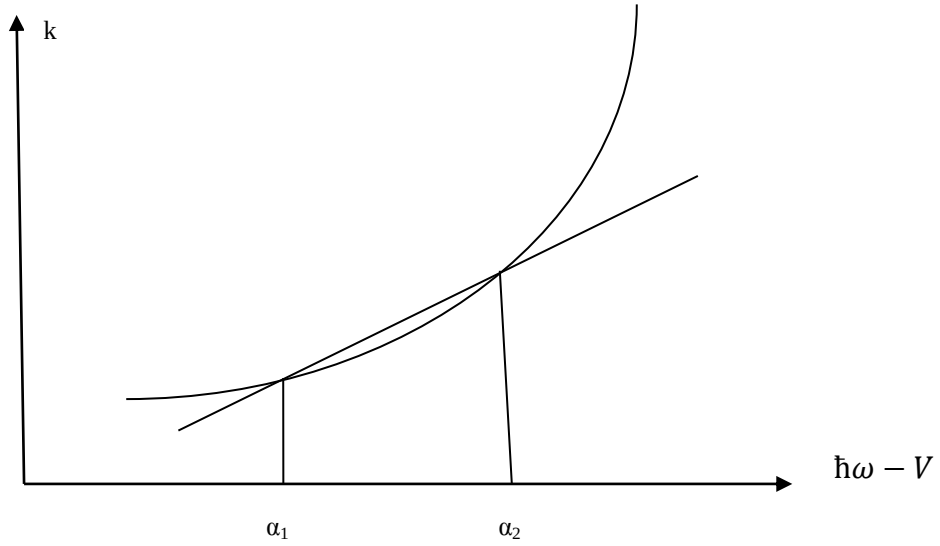

fig 2.5: Schematic of the linearization process of the dispersion relation. Note the line should coincide with the function and this is possible only on a narrow range (α_1 α_2 are the intersection point extracted accordingly).

The correspondence of $\frac{\partial}{\partial t} = -i\omega$ and $\frac{\partial}{\partial x} = ik$ leads us to rewrite equation (2.18) into the partial differential equation:

$$i\hbar\frac{\partial}{\partial t}\psi(x,t) = \left(-i\hbar\frac{1}{g_1\partial x} + V - \frac{g_2}{g_1}\right)\psi(x,t) \tag{2.19}$$

Now we outline how to incorporate the ABC into the lattice representation of the wave function (with ħ = m = 1). The idea is to replace the differential equation for the boundary components ψ_N^n and ψ_1^n of the state vectorψ^n. In order to obtain an accurate expression for the derivative at the borders of the grid, it is convenient to introduce an intermediate point$\hat{x}$ between thelast two points of each side of the grid, then for example, at the right-hand side thewave function must be replaced by

$$\psi(\bar{x},t) \simeq \frac{1}{2}[\psi(x_N,t) + \psi(x_{N-1},t)] \tag{2,20}$$

In the grid representation, the finite difference equation for the right- and left-hand sides reads respectively:

$$\begin{aligned}\frac{i}{2\Delta t}(\psi_N^{n+1} + \psi_{N-1}^{n+1} - \psi_N^n - \psi_{N-1}^n) \\ = \frac{-i}{g_1\Delta x}(\psi_N^n - \psi_{N-1}^n) + \frac{1}{2}\left(V - \frac{g_2}{g_1}\right)(\psi_N^n + \psi_{N-1}^n)\end{aligned} \tag{2.21}$$

and

$$\frac{i}{2\Delta t}(\psi_2^{n+1} + \psi_1^{n+1} - \psi_2^n - \psi_1^n) = \frac{-i}{g_1\Delta t}(\psi_2^n - \psi_1^n) + \frac{1}{2}\left(V - \frac{g_2}{g_1}\right)(\psi_2^n + \psi_1^n) \qquad (2.22)$$

Equations (2.21) and (2.22) allow a straightforward incorporation into the matrix representation. The new matrices $D_{1,2}$ are given by:

$$D_1 = \begin{pmatrix} \eta_4 & \eta_3 & & & & \\ \alpha & \gamma_2 & \alpha & & & \\ & \alpha & \gamma_3 & \alpha & & \\ & & \ddots & \ddots & \ddots & \\ & & & \alpha & \gamma_{N-1} & \alpha \\ & & & & \eta_3 & \eta_4 \end{pmatrix}$$

$$D_2 = \begin{pmatrix} \eta_2 & \eta_1 & & & & \\ -\alpha & \xi_2 & -\alpha & & & \\ & -\alpha & \xi_3 & -\alpha & & \\ & & \ddots & \ddots & \ddots & \\ & & & -\alpha & \xi_{N-1} & -\alpha \\ & & & & \eta_1 & \eta_2 \end{pmatrix} \qquad (2.23)$$

$$\eta_2 = \eta_1 = \frac{i}{2\Delta t} \qquad (2.24)$$

$$\eta_3 = \frac{i}{2\Delta t} + \frac{i}{g_1\Delta x} + \frac{1}{2}\left(V - \frac{g_2}{g_1}\right) \qquad (2.25)$$

$$\eta_4 = \frac{i}{2\Delta t} - \frac{i}{g_2\Delta x} + \frac{1}{2}\left(V - \frac{g_2}{g_1}\right) \qquad (2.26)$$

Let us write the matrix product as:

$$E = D_2^{-1}D_1 \qquad (2.27)$$

The main cause of artificial back reflection for plane waves in the presence of the above boundary conditions comes from the approximate nature of the finite difference evaluation. Clearly, these approximations become better decreasing for the grid spacing Δx.

VI. Perfectly matched layers

The perfectly matched layer (PML) is an absorbing layer, for which a modified set of equations are solved in the layer. The significant feature of the PML in contrast to a general absorbing layer is the perfect matching, which guarantees that the continuous PML is non-reflecting at the interface to the interior domain for all frequencies, and all incoming angles in the multi-dimensional case. However, discretization introduces numerical reflections at the interface.

The PML method was developed for Maxwell's equations in electromagnetics, and is widely used for hyperbolic problems in general. The PML approach has been used also for the Schrodinger

equation, but the extent of the investigations is far from that of hyperbolic PMLs. A common approach for the TDSE is the modal ansatz PML, where the starting point of the PML derivation is modal solutions in the frequency domain. An alternative way is to introduce a coordinate change, as in the case of ECS and SES. For most hyperbolic problems, the modified equations in frequency domain cannot be transformed back into time-domain without the introduction of auxiliary variables, which leads to additional equations in the system. However, no auxiliary variables need to be introduced for the Schrodinger equation. Thus, when solving the TDSE with PML no additional equation needs to be solved. However, extra computational effort is required, compared to the solution with ABC, due to the additional grid points in the layer. On the other hand, compared to ABC the PML formulation is easier to extend to multi-dimensional problems. Application of PMLs have also been made to the nonlinear TDSE, where we construct a PML for a system of two-dimensional coupled nonlinear Schrodinger equations with mixed derivatives. Due to the mixed derivatives, waves with opposite phase and group velocities are supported. For many hyperbolic problems, this would lead to unstable layers, in the sense of exponentially growing solutions for the continuous problem. Here, however, it only leads to a stability condition on the layer parameters. Stability analysis for Schrodinger PMLs is an area of research which needs more consideration. However, stability problems have not been observed for the TDSE without mixed derivatives. In order to derive a PML of the Schrödinger equation , we need to make the assumption that the potential is independent of x, i.e. V (x, t) = V (t). For the multi-dimensional case, the requirement is that the potential in the layer is independent of the normal direction in which the PML is imposed, but it can depend on other spatial variables. By performing the coordinate transformation

$$x \to x + e^{i\gamma} \int_{\pm x_0}^{x} \sigma(\omega) d\omega, \qquad |x| \geq x_0 \tag{2.28}$$

By introducing this transformation in the Schrodinger equation we arrive at the PML equation:

$$\begin{cases} i\hbar \dfrac{\partial \psi(x,t)}{\partial t} = -\dfrac{\hbar^2}{2m} \dfrac{1}{1 + e^{i\gamma}\sigma(x)} \dfrac{\partial}{\partial x} \left(\dfrac{1}{1 + e^{i\gamma}\sigma(x)} \dfrac{\partial \psi(x,t)}{\partial x} \right) + V(t)\psi(x,t) \\ \psi(-x_0 - d, t) = \psi(x_0 + d, t) = 0, \\ \psi(x,0) = \psi_0(x), \end{cases} \tag{2.29}$$

The absorption function σ(x) is a nonnegative, real function in $[-x_0 - d, -x_0] \cup [x_0, x_0 + d]$, and zero in $[-x_0, x_0]$, and γ should be in the range $0 < \gamma < \pi/2$.

Perfect matching means that there are no reflections at the interface. This is achieved if $\sigma(\pm x_0) = 0$, since it implies continuity of ψ and ψ_x at the interface. In the continuous setting, the

damping introduced by the PML depends only on the value of the integral in (2.29), due to the perfect matching property. Hence, a large value of the integral results in a large damping, and allows the use of a thin layer. However, the case is different for the discretized problem and $\sigma(x)$ needs to be chosen carefully in order to avoid numerical reflections. Thus, a balance between a sufficiently steep slope of $\sigma(x)$, such that the width of the PML can be kept small, and a sufficiently smooth function in order to avoid numerical reflections is advisable.

VII. Summary

It is clear from this short review that the problem of the suppression of the unwanted numerical reflection at the boundary is far from being solved. The bunch of proposed solutions, are partially satisfactory and the unified solution if it exists really, is still to be established. However we can conclude that all the efforts in this direction are providing continuously more accuracy and more portability of the proposed solutions. In our investigation we are going to limit the calculation to the simplest approaches and try to elaborate a conclusive comparison

Chapter 3: Numerical implementation and evaluation

I. Introduction

In this last chapter we are interested in establishing a comparative study between different suppression methods. The aim is to shed light on the advantages and inconvenient of some of these methods and thereby evaluate their effectiveness. Before that it is important to establish a program that resolves the time dependant Schrodinger equation. For that, the conventional Cranck- Nicolson method is exploited. We are using FORTRAN software to perform the coding with the help of LAPACK library for the matrix inversion and multiplication.

II. Coding strategy and implementation

To translate the numerical results established at the end of the previous chapters we are using FORTRAN software for the coding and the LAPACK libraries for the routines of inversion, matrix-matrix product and matrix-vector product. Besides being very commonly used by the physicists community, the FORTRAN software is a very versatile language allowing through its object orientation and low structure plenty of manipulations that are not possible with other highly structured languages. When FORTRAN coding is coupled with LAPACK libraries which are ready-to-use FORTRAN routines, coding becomes easier and more compact.

The program includes an input part where we assign values to some parameters whether physical or needed for the structure of the program as for example the parameters for the initial wave packet, assignment of matrices elements of the Hamiltonian… and the spatial and temporal paces (Δx and Δt)… we first evaluate the inverse matrix D_1^{-1} and then the matrix-vector product $(1 - 2D_1^{-1})\psi$. For each iteration, the wave packet function is multiplied by the resultant matrix to promote the result to the next instant. Where for these operations we are using the complex-valuated routines: cgetrf,cgetri and cgemmv. These different operations could be summarized by the flowchart of figure 1.

The program is outputting formatted files for gnuplot. It is possible then to create an animation that allows the observation of the evolution of the wave packet across time. Only snapshots of this evolution are captured in our figures to sketch the main features of the process. Notice that the values of the parameters are given in atomic units (a.u) so we omit the mention of the unit for most of the stated values.

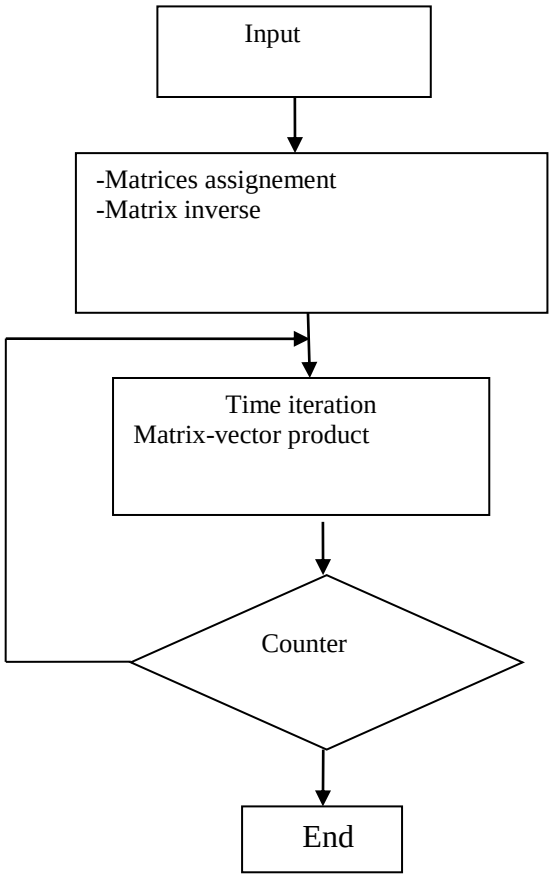

fig 3.1. flowchart of the elaborated program

III. Calculation at the boundary

First let us show explicitly the problem we are encountering at the edge of the numerical box when no appropriate conditions are implemented to handle the reflection occurring at the boundaries. The figure .3. 2 below represents snapshots of the evolution of a wave packet before and after the impact at the edge in case where no condition is imposed at the edge. The calculation is performed for a free (the potential is nil) and a normalized Gaussian wave packet with a variance σ=1.0 and for a momentum p=10 u.a. We are considering also Δx=0.1 and Δt=0.0002. We can notice that once the wave reaches the edge, it is completely reflected as if impinging on an infinitely high barrier. This is a numerical problem related to the size of the box as in reality the wave should evolve to infinity. We can see as in figure 3.3 and 3.4 that changing the energy of the wave (consequently p) changes a little to the problem and only the interference pattern is more complex for higher energy.

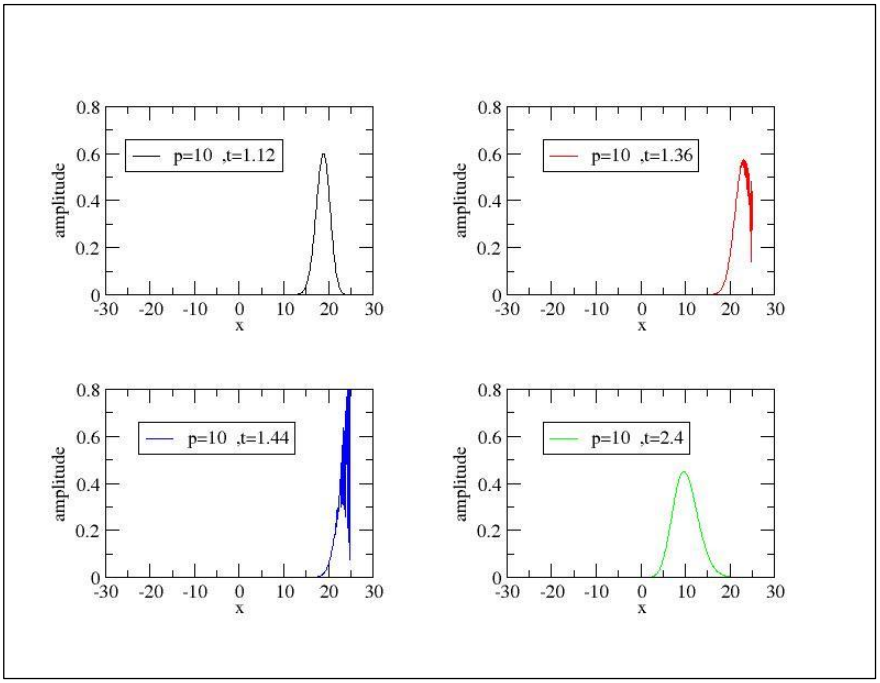

fig 3.2: Snapshots of a free Gaussian wave packet with no condition imposed at the edges. We have p=10.

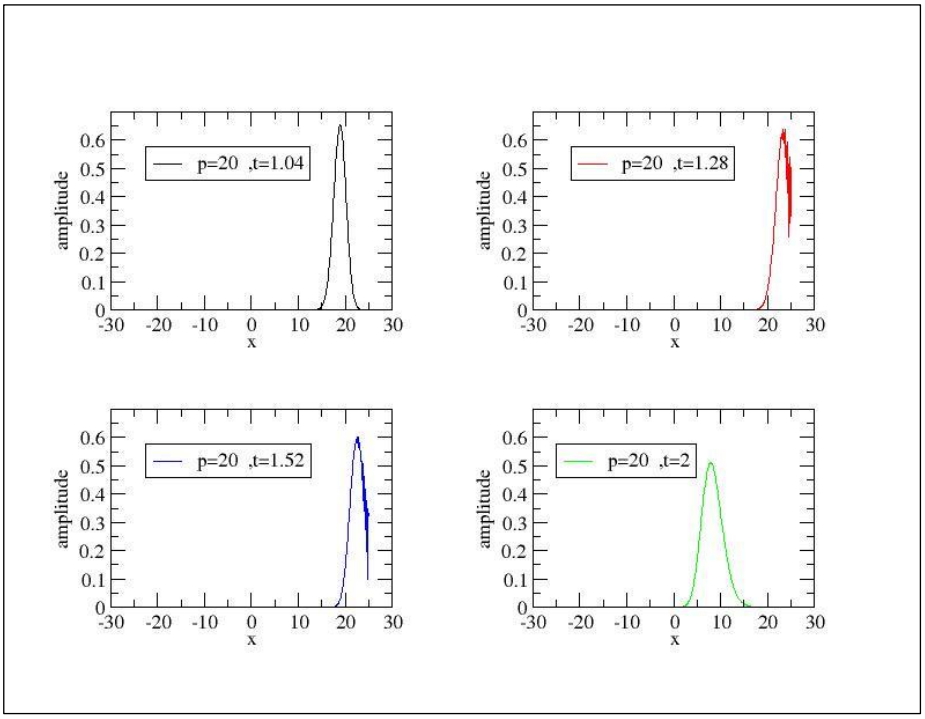

fig 3.3: The same as figure 3.2 for p=20

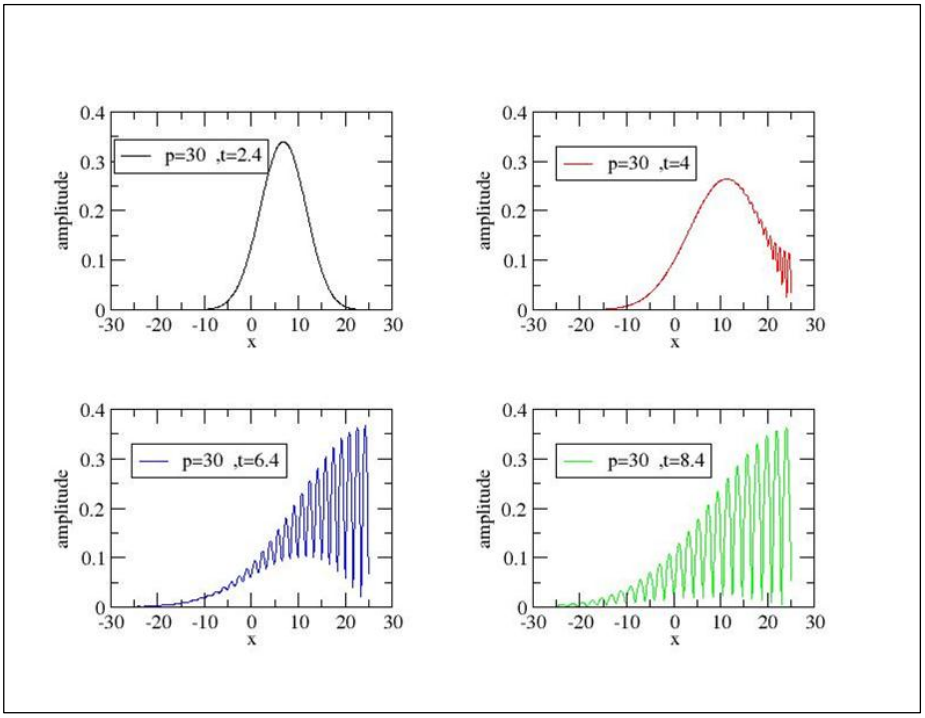

fig 3.4: The same as figure 3.2 for p=30

IV. Masking method

As seen in the previous section the reflection at numerical box edge is an artifact that could contaminate the physical results in this region of the space. We can extend the numerical box to the range where no interference is possible but this will unavoidably mean more memory resources that sometimes we are not able to afford. The simplest way to get rid of this reflection is masking the wave at the edge. For this we are going to check the effectiveness of some masking functions. The mathematical expressions for these mask-functions are given below and are depicted on figure 3. 5. These are decreasing function from the threshold value of one and the main difference between these function is their relative slope. We are going to analyze how these masks are affecting the back reflection and this is done by illustrating snapshots before and after the impact on the edge. The time of each capture is accordingly indicated.

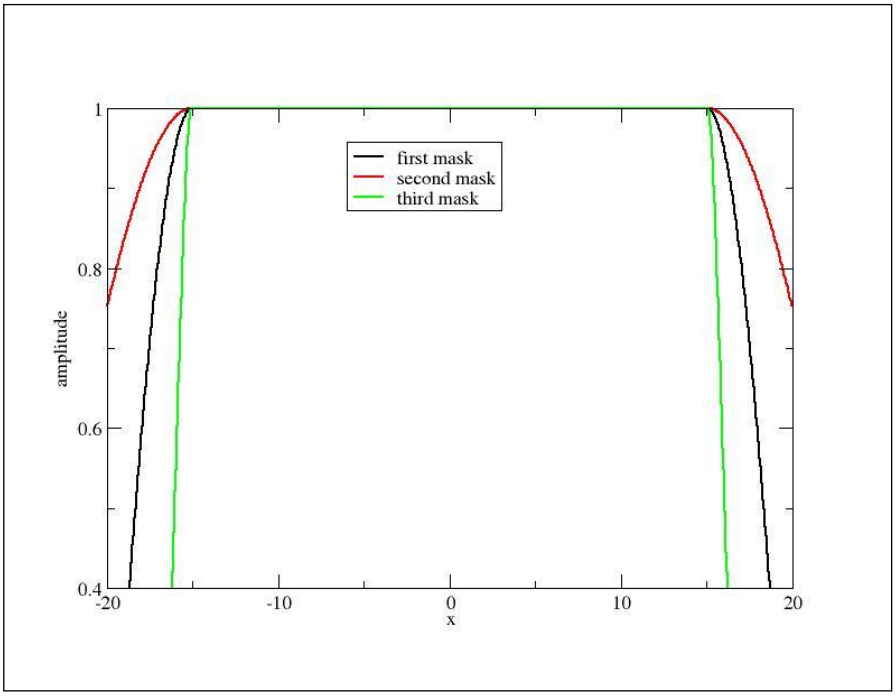

fig 3.5: Comparison of the different masks

IV.1 First mask:

Firstly we are considering a cosine function given by:

$$f(x) = cos\left(\pi \frac{|x - x_0|}{2(x_{max} - x_0)}\right)^{\frac{1}{\alpha}} \tag{3.1}$$

x_{max} is the edge of the box taken here to be 30 u.a and $x_0$is the point where the mask starts to affect the wave function (considered here to be 2/3 x_{max}). α is an exponent that control the smoothness of the slope of the function and hence can improve the transmission. Taking α=1, we can see in figures 3. 6 and 3.7 that this first masking function is effective in reducing refection until p=70 a.u and then refection starts to reappear for higher energies as in figure3.8 for p=75.

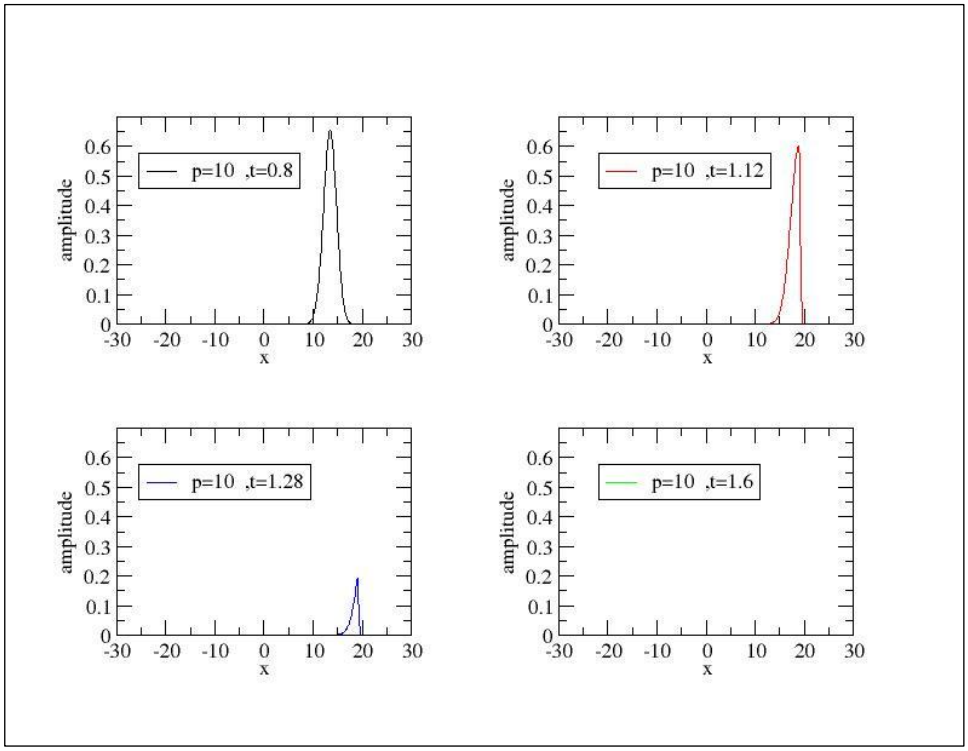

fig 3.6: Snapshots of the Gaussian wave packet in case where the first mask is implemented (α=1, p=10). The mask is set at *x*=20. The wave has completely disappeared in the last figure proving the effectiveness of the mask at the indicated energy

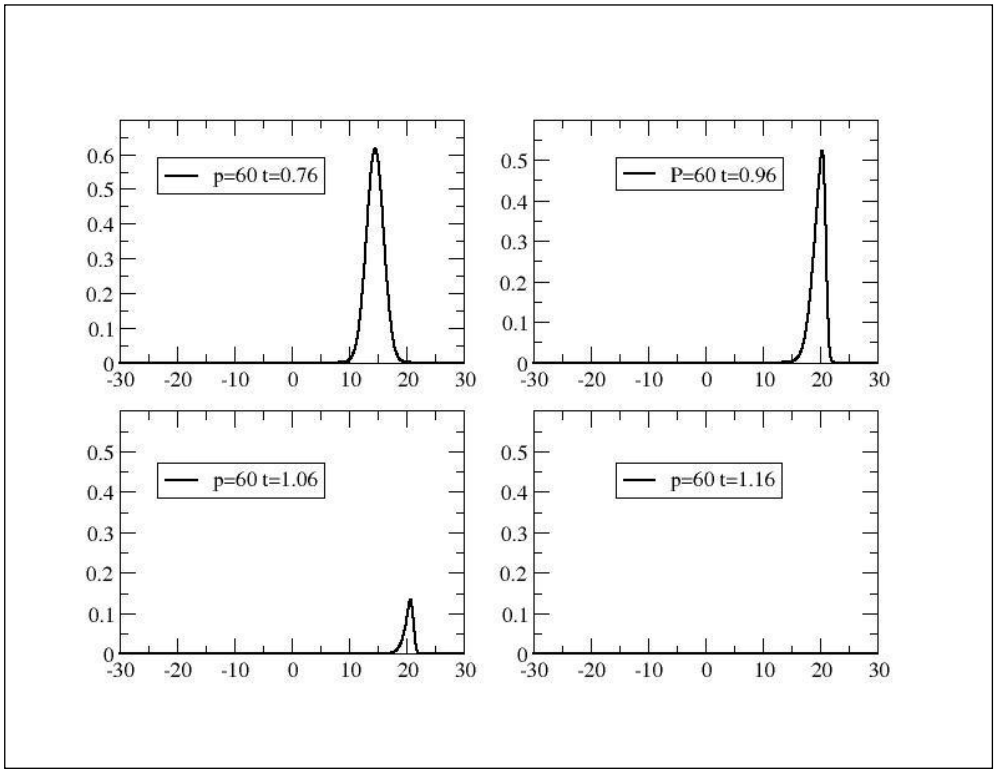

fig 3.7: The same as figure 6 for α=1 and P=60 a.u

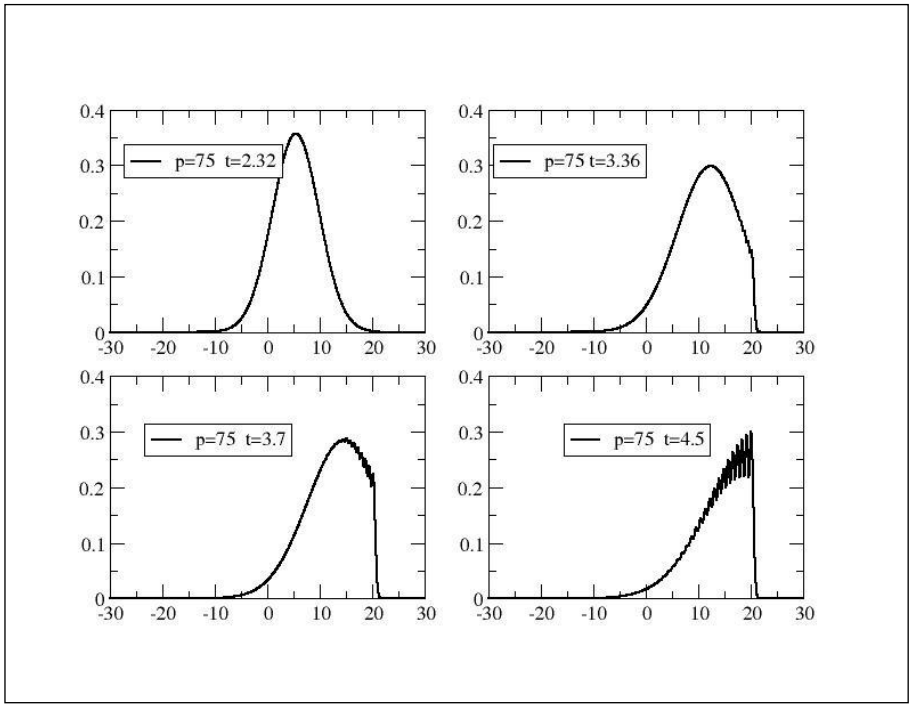

fig 3.8:The same as figure 6 for α=1 p=75 a.u

We checked if changing the exponent α to 8 can improve the situation for the last calculation and we can see on figure 3.9 that this attenuates the wave to a better rate without reaching the complete cancellation. We can conclude that the exponent can contribute to the improvement of the effectiveness of the first mask.

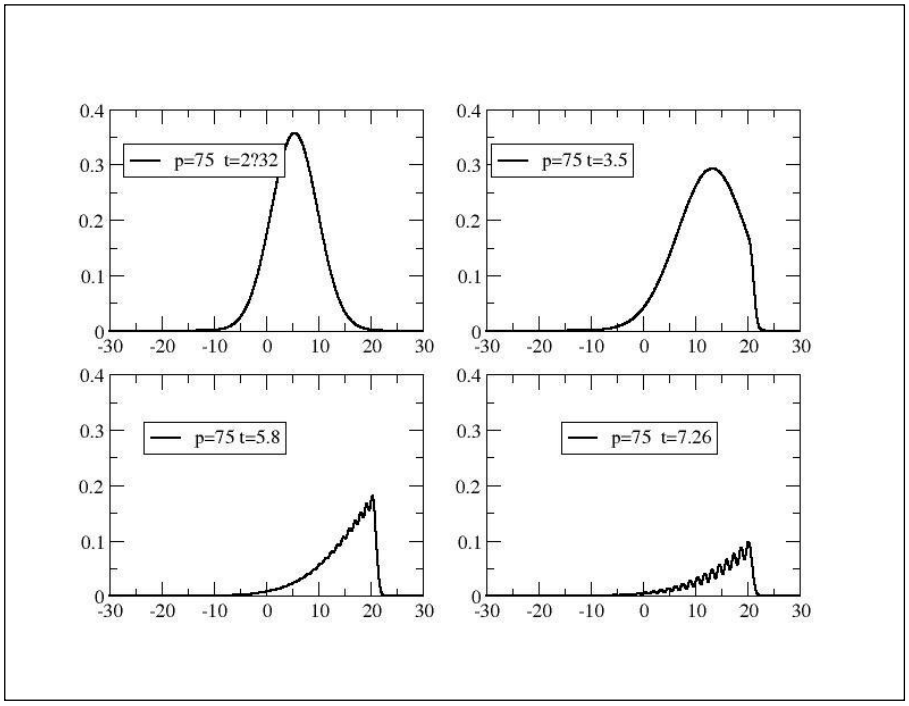

fig 3.9. Same as figure 6 for α=8 p=75 a.u

IV.2 Second mask:

Let us check the results in the same manner for another masking function given as:

$$f(x) = \alpha\left[sin^2\left(\frac{\pi x}{2x_0}\right)\right] \tag{3.2}$$

Where α is equal to 1. Here also we can notice that the mask is effective at low energy as in figure 3.10 and3. 11 and loses effectiveness for high energy as in figure 3.12.

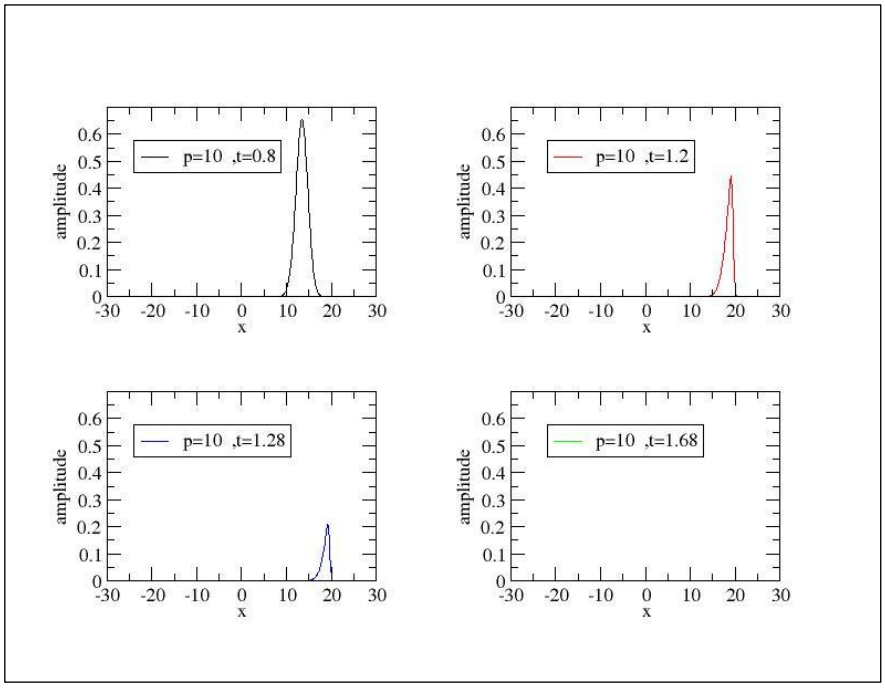

***fig 3.10*:** Snapshots of a Gaussian wave packet in the case where the second mask function is implemented at the edge for p=10. The last figure is indicating the complete cancelation of the wave packet

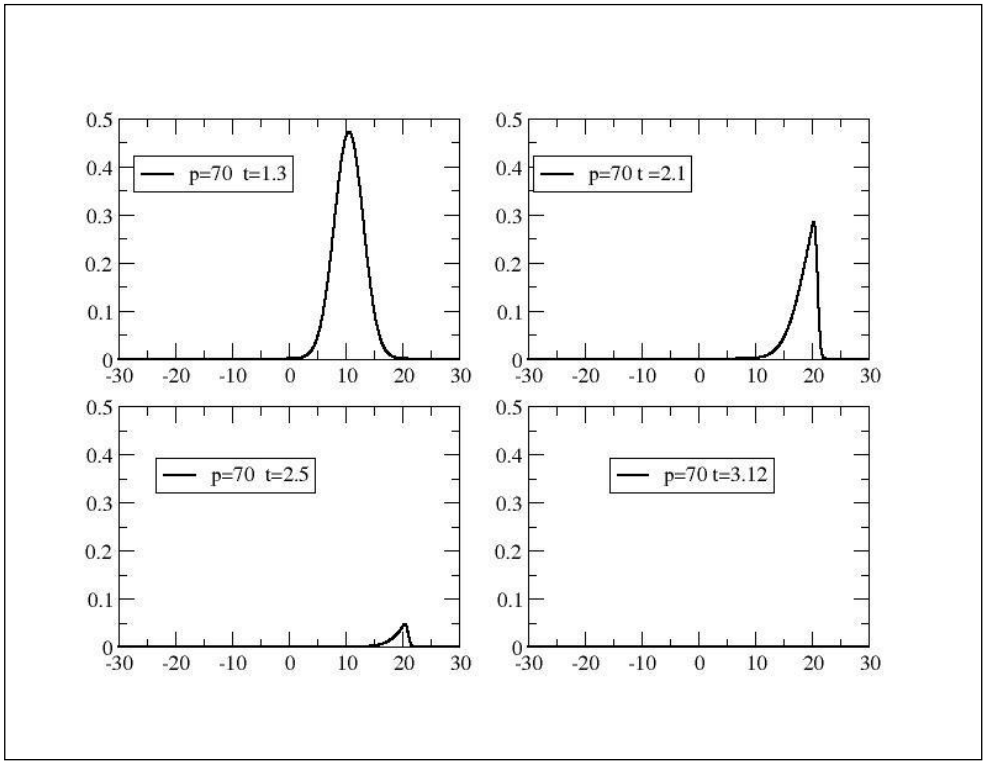

fig 3.11:The same as figure 10 for p=70

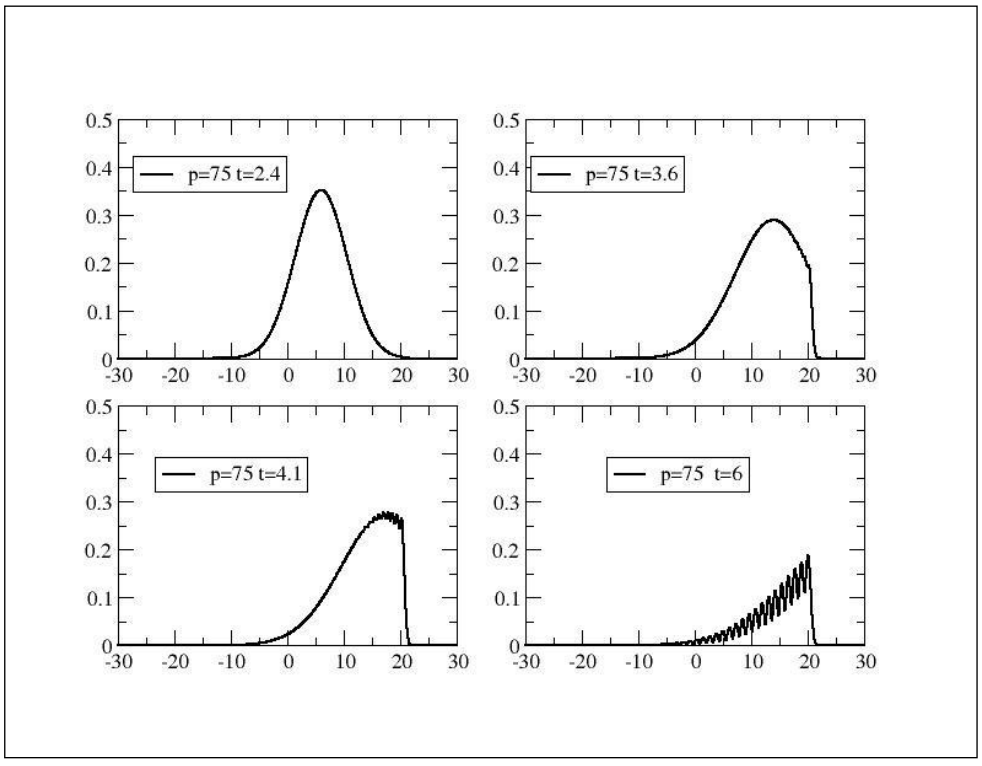

fig 3.12: The same as figure 10 for p=75

IV.3 Third mask:

Similar to the second mask but with a higher exponent, we are checking the results of a third mask function given by:

$$f(x) = sin^4\left[\pi \frac{(x-x_{max})^2}{2x_b}\right] \qquad (3.3)$$

The results are however similar to the second mask and the exponent being affecting only the interference pattern at the edge (figures 3.13, 3.14 and 3.15) which is the result the different slopes.

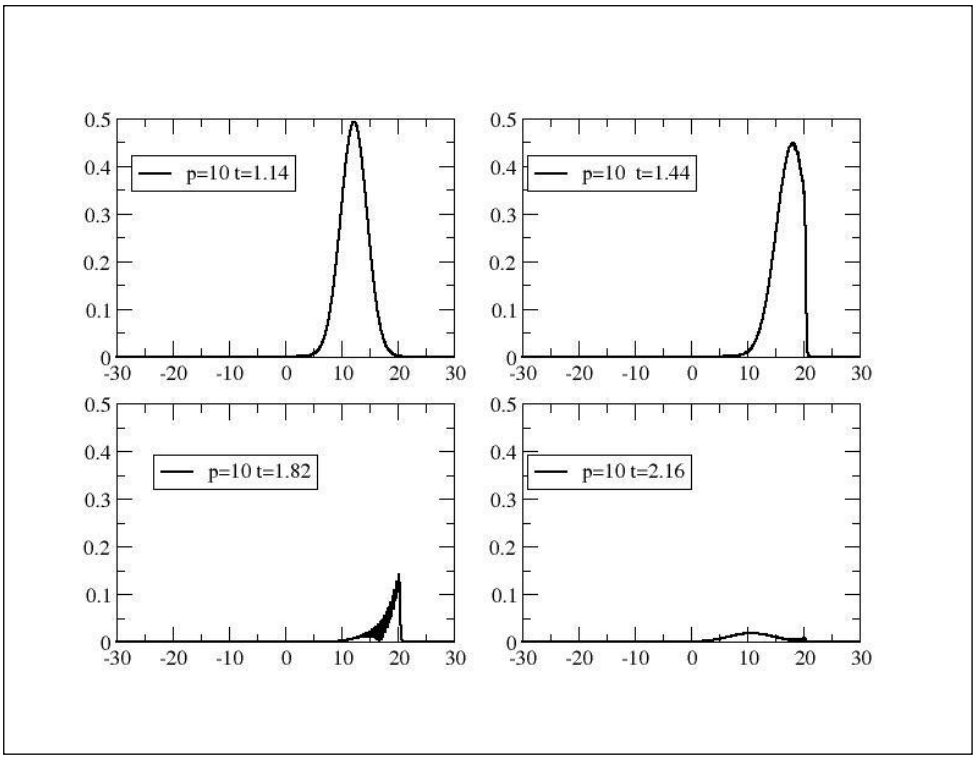

fig 3.13: Snapshots of a Gaussian wave packet in the case where the third mask function implemented at the edge for p=10

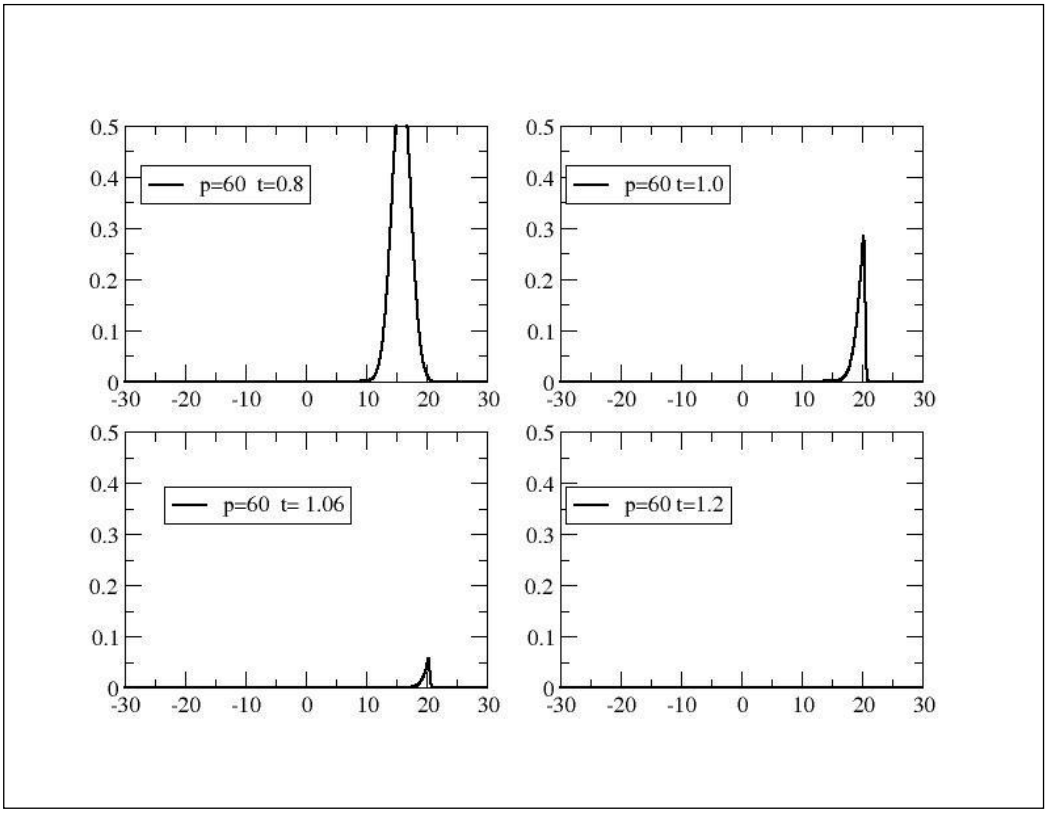

***fig 3.14*:** The same as figure 13 for p=60.

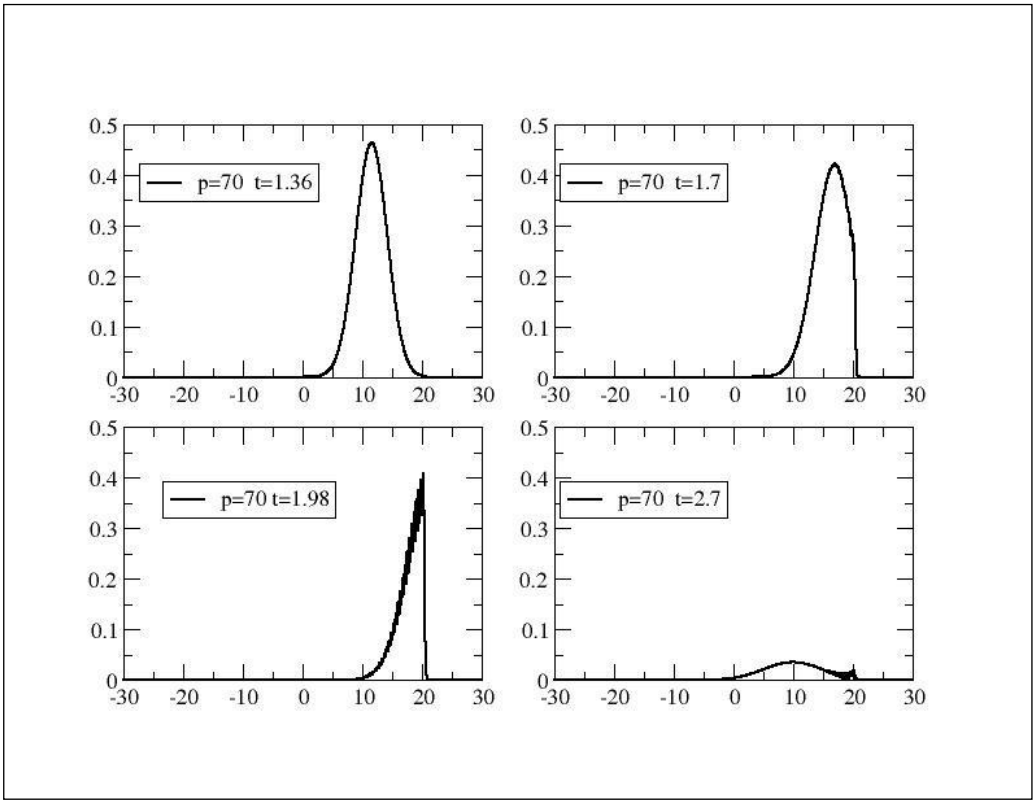

***fig 3.15*:**The same as figure 13 for p=70

In conclusion, despite the fact that the masking technique is very easy to implement as it is just a product of the masking function and the wave function, it presents the inconvenient of being non local as it needs an interval non negligible of the numerical box to be effective. This implies a proportion of the memory devoted to convey this constraint. It presents also the inconvenient of being non effective at high energy. The whole method suffers from the absence of a clear quantative criteria in order to assert of the convenience of different masks and it becomes just a matter of "try and see". We can notice that the back reflection for high energy is due to the fit between the slope of the masking function and the momentum.

V. The complex absorbing potential:

We move now to another technique for the reflection suppression which is the use of a negative complex potential. Introduced in the Hamiltonian expression, this potential will act as an attenuation that will affect the whole wave amplitude at each time iteration. This method is also non local as it needs an interval on which the potential will act on the wave function. To test this method we propose three expressions for the complex potential: the quadratic, the quartic and single exponential potentials. The mathematical expressions for these potentials are given below and their different shapes are compared in figure 3.16. All of these potentials are highly negative and the most important difference is their decreasing rate, the quartic potential having the most dramatic decrease and the single potential the most gentle one. This is more clearly apparent in the attenuation curve which is the exponential of the potential value. We can see on figure 3.16 that the situation is reversed as the exponential potential decreases gradually and have the time to affect in a more important manner the amplitude of the wave packet.

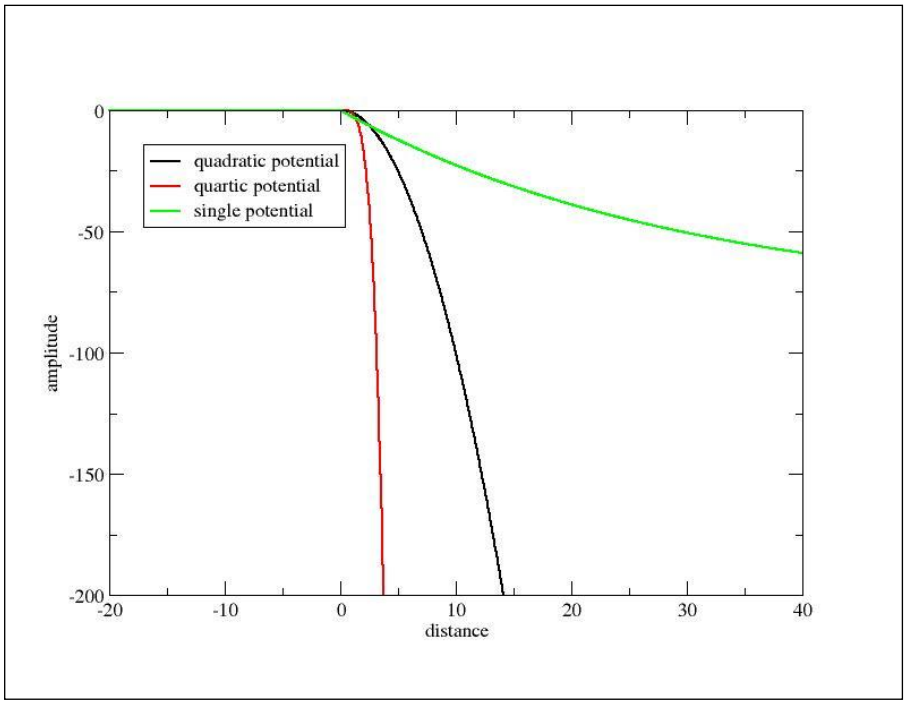

fig 3.16. Comparison of the different potentials

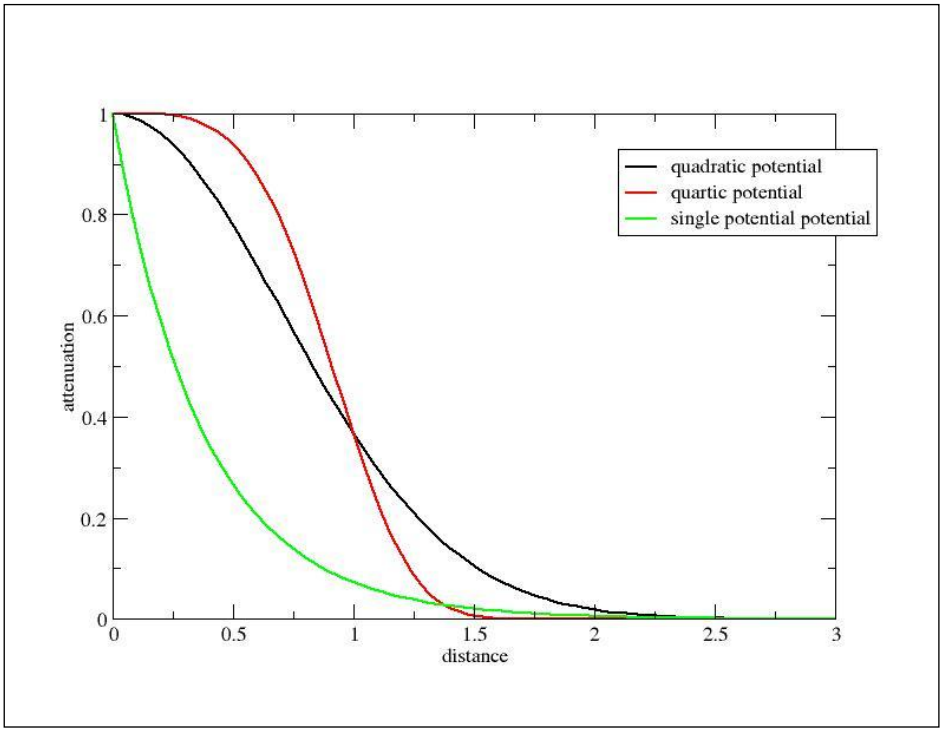

fig 3.17. Comparison of the potentials attenuation

V.1 Quadratic complex potential:

For this case the potential is given as:

$$-i\alpha^2(x - x_0)^2 \qquad (3.4)$$

Where α is a factor considered to be equal to one and x_0 is the point where the potential starts to affect the wave function where we consider $x_0 = 0.0$. We are setting the damping potential on only one side of the box and we are extending the edge on one side to 40.

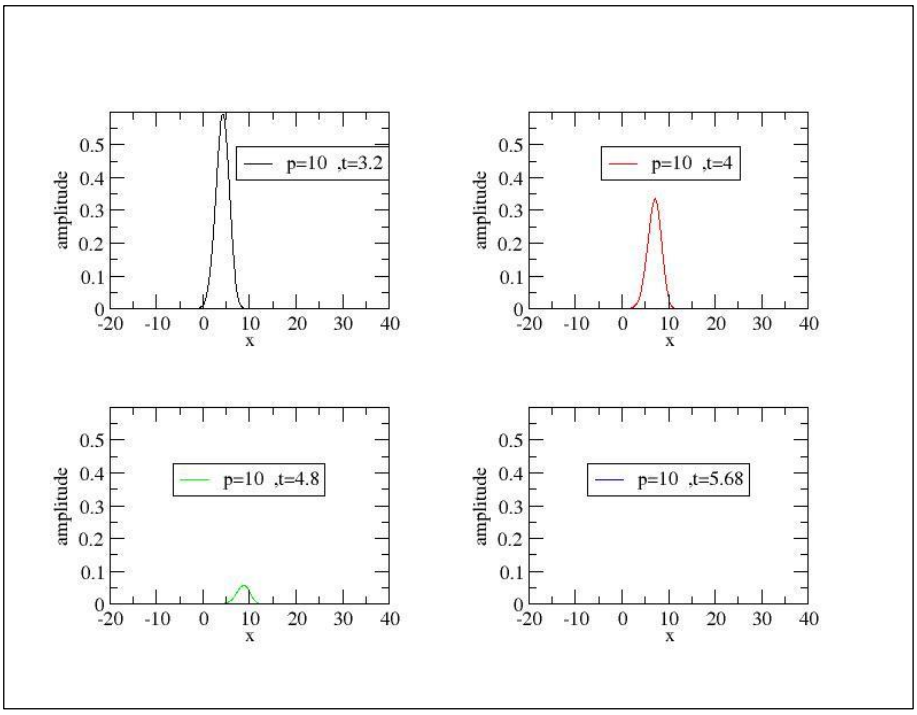

Fig.3.18: Snapshots of Gaussian wave packet evolution in case where a quadratic complex potential is implemented at the edge, p=10.

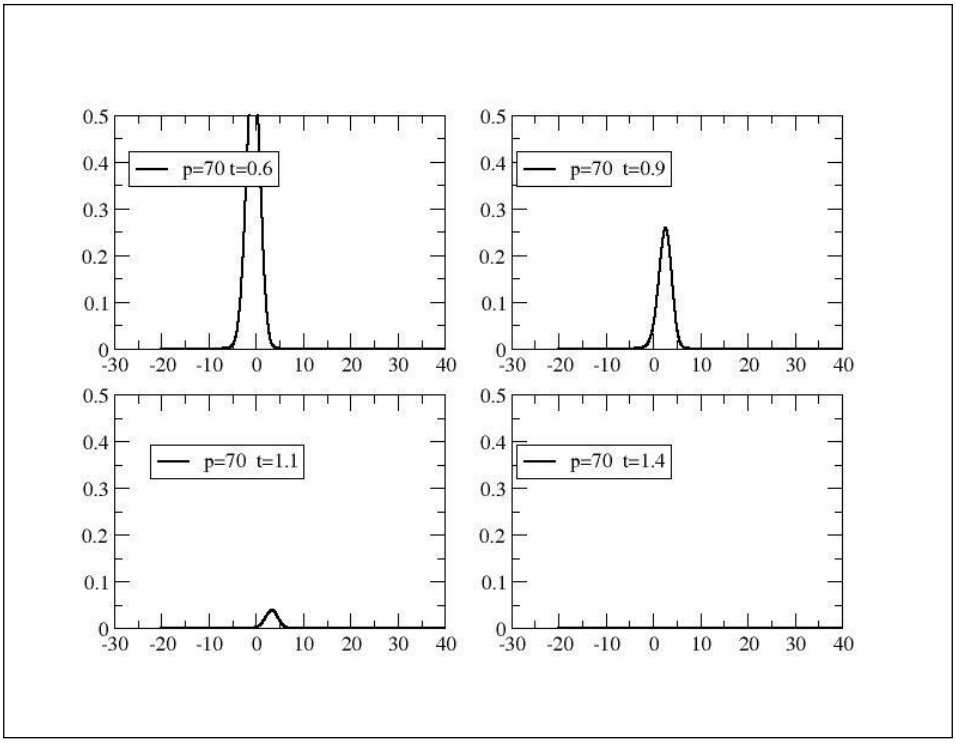

fig.3.19: The same as figure 18 with p=70.

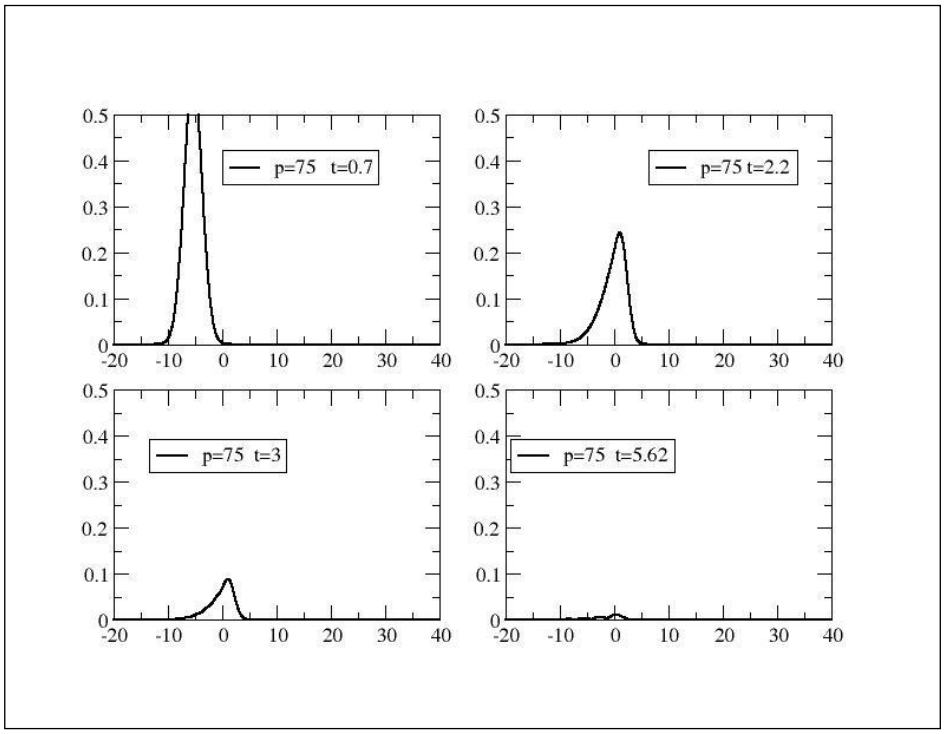

fig 3.20 : The same as figure 18 with p=75.

We can see through the figures 3.18 and 3.19 that the energy range on which the suppression is effective is more important since we can extend the value to p=75 u.a. The space range on which the potential is effective is comparable to that of the masking method (around 10).

V.2 Quartic complex potential :

The expression of the second potential we are testing is given by:

$$-i\alpha^2(x-x_0)^4 \qquad (3.5)$$

The results of the attenuation of the reflection for different energies are illustrated on figures 3.21 and 3.22. The energy and the spatial range is comparable to those of the quadratic potential but the attenuation of the wave is extended on the whole spatial range in rather more "gentle" effect.

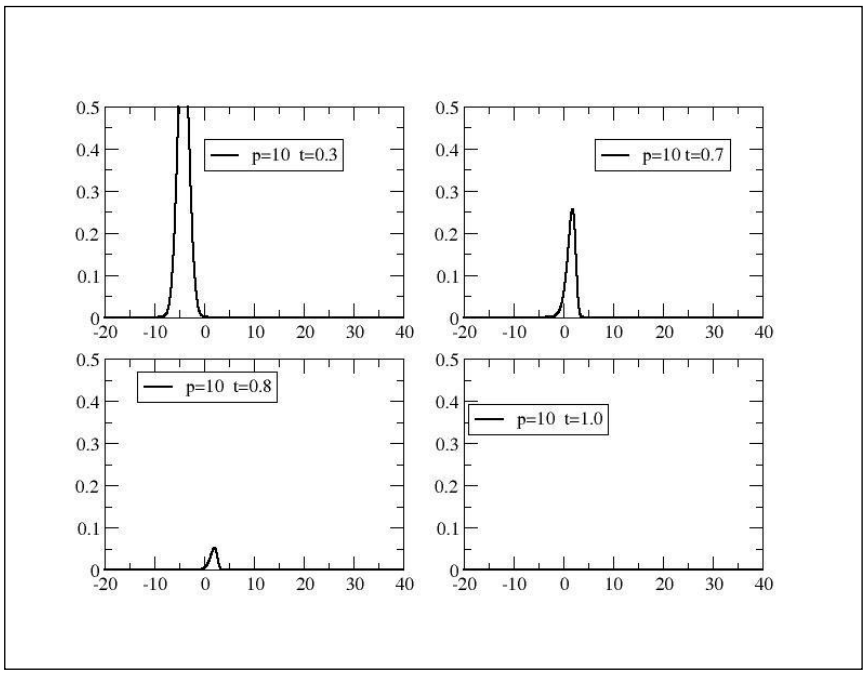

fig 3.21: Snapshots of wave packet evolution in case of the quartic potential p=10

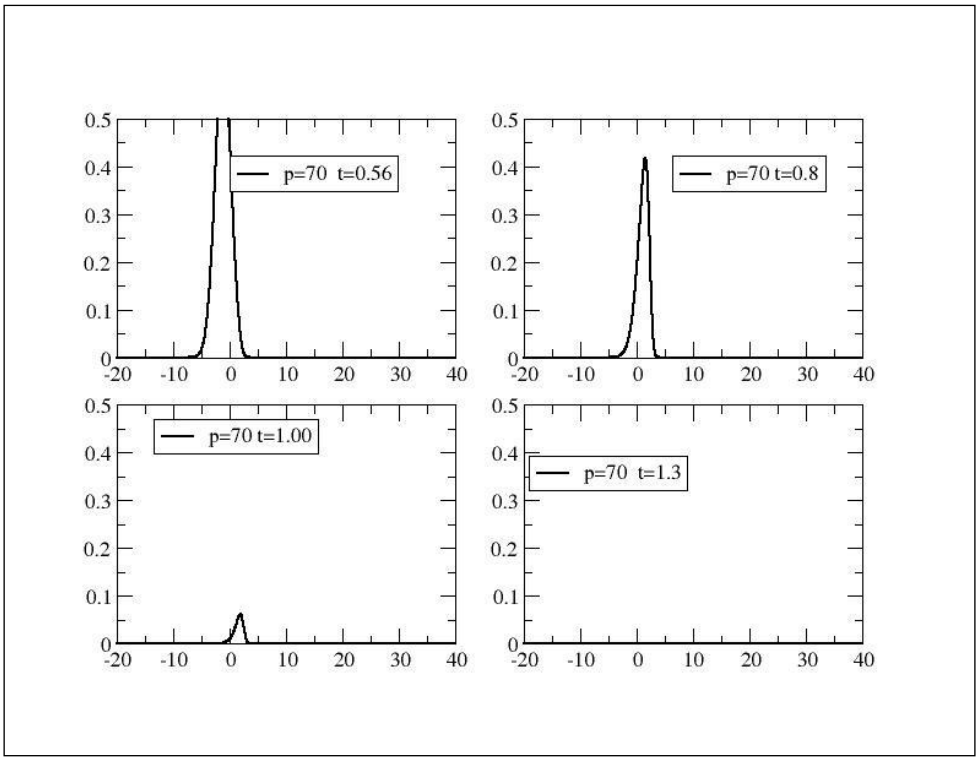

fig 3.22: The same as figure 21 for p=70.

V.3 Single exponential complex potential:

The third potential is expressed as:

$$-i\alpha^2\left(1 - e^{(-x/\beta)}\right) \qquad (3.6)$$

The expression of this potential is constructed in such way to assure continuity at x_0 and for this we are setting α =80 and β=30.

We can notice that the single exponential absorbing potential records are quite similar to the two other potentials with regards to the energy effectiveness and the spatial range. Nonetheless this method is reaching similar results in a smaller time which is due to the quick attenuation introduced by this potential.

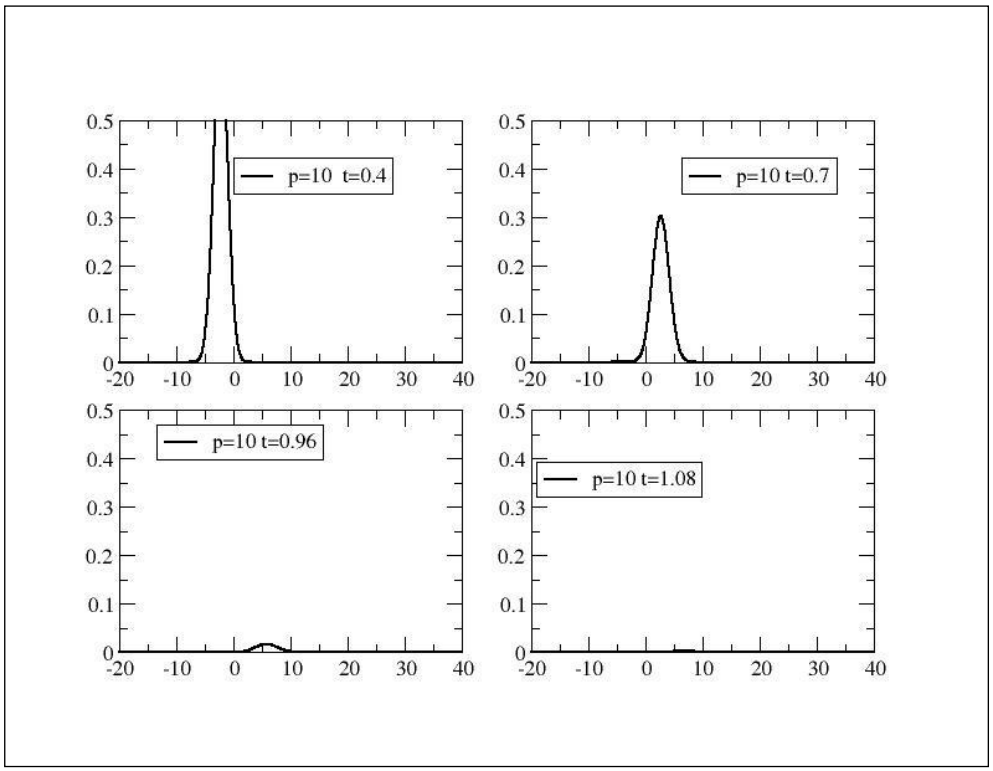

fig 3.23: Snapshots of wave packet evolution in case of the single exponential complex potential p=10

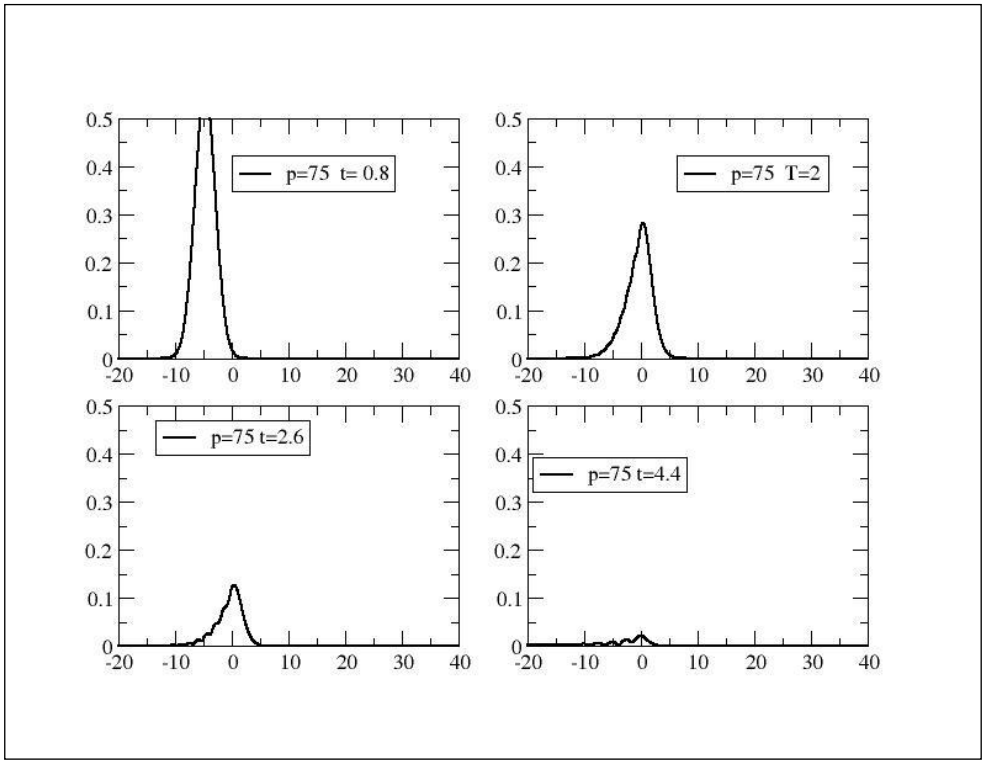

fig 3.24: The same as figure 23 for p=75.

VI.3 Absorbing boundary Conditions:

We study now t another category of suppression methods which are local by nature (no need for a spatial range for the method to be effective) and more particularly we are studying the absorbing boundary conditions method. As introduced in chapter 2, the method is approximative and is based on the rationalization of the dispersion relation to accommodate one way wave at the right and the left edge of the box. The Hamiltonian matrix in the program should be changed accordingly and for this we are using the following constant values (α_1=24 and α_2=25) and g_1 and g_2 are calculated according to the formulas

$$g_1 = \mp\frac{\sqrt{2m\alpha_2}-\sqrt{2m\alpha_1}}{\alpha_2-\alpha_1} \quad , g_2 = \mp\frac{\alpha_2\sqrt{2m\alpha_1}-\alpha_1\sqrt{2m\alpha_2}}{\alpha_2-\alpha_1} \tag{3.7}$$

We can see straightforwardly on figure 3.25 that this type of condition simulates more naturally the outgoing wave for p=7. However the effectiveness of the method start to break gradually around a narrow range of energy as seen in figures 3.26 and 3.27 for p=10 and p=13 respectively. Consequently the constant of linearization should be tailored for a narrow interval of energy separately. The major advantage of this method is that it does not any space interval and is practically a point-method.

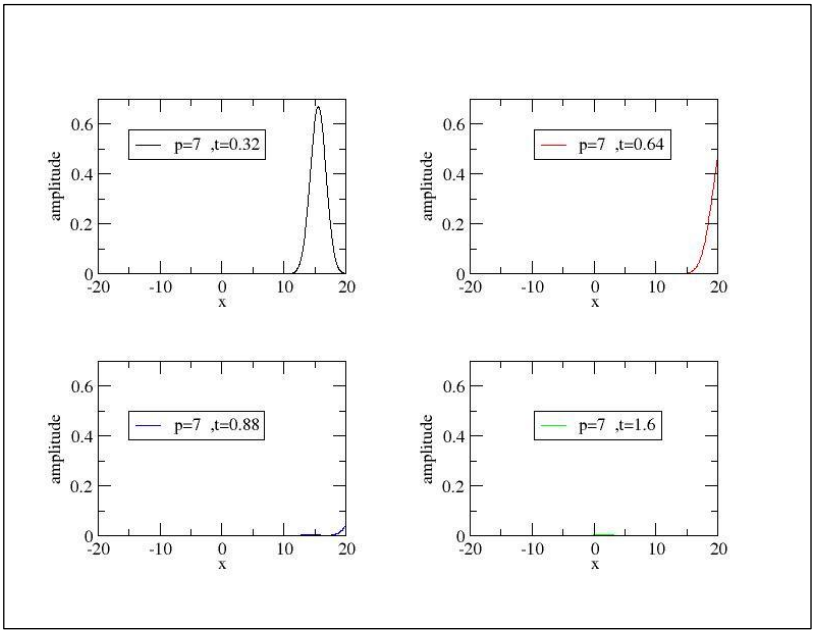

fig 3.25: Snapshots of wave packet evolution in case the ABC's method for p=7

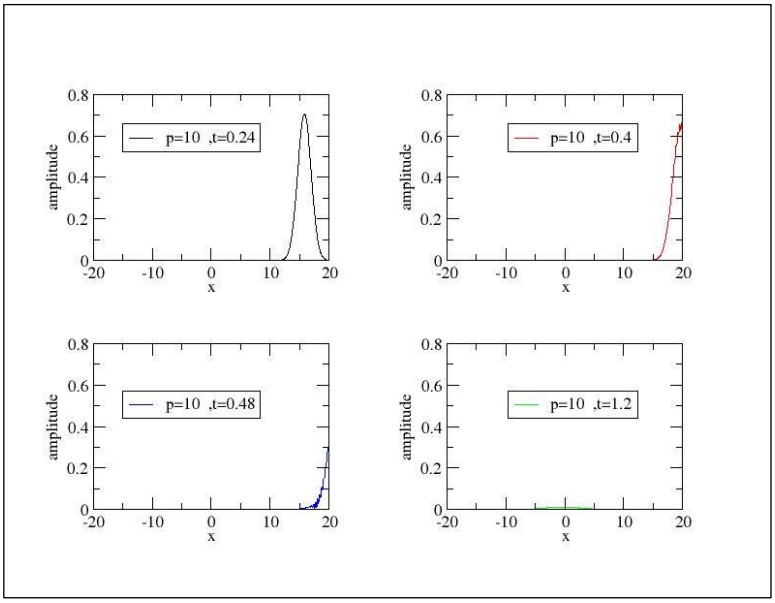

fig 3.26: The same as figure 25 for p=10

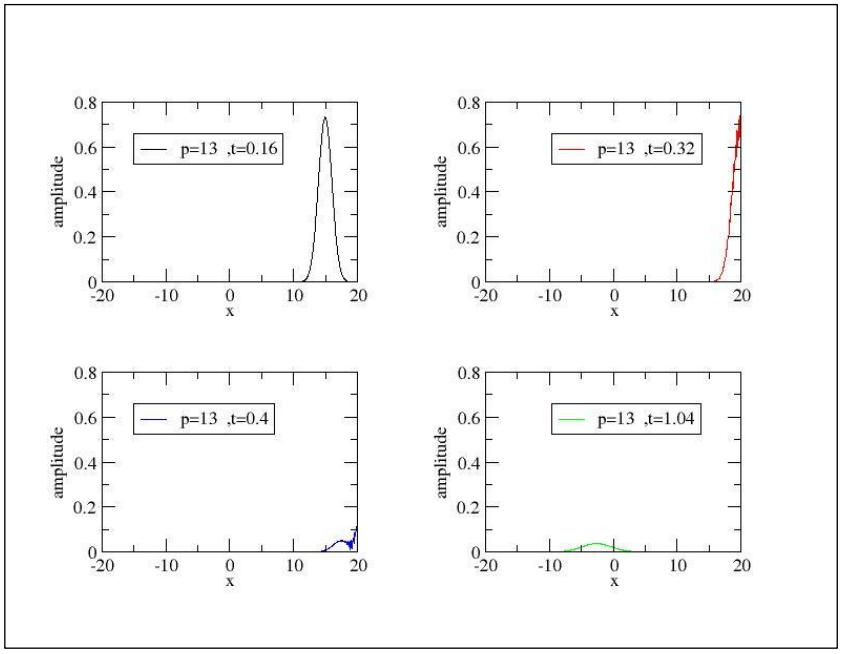

fig 3.27: The same as figure 25 for p=13

Conclusion

A numerical solution to the Schrodinger equation is an unavoidable choice in numerous physical cases of interest, if we are attempting to extracte eigenvalues and eigenvectors that highlight the most important features of the quantal system. To reach a numerical solution to the Schrodinger equation, many methods are devised, each with its own advantages and inconvenient. In our study we opted for the Crank-Nicolson method as it is a simple and a stable one. In addition it is a method which is less memory demanding as compared to other methods.

Understanding the numerical approach of Crank-Nicolson allowed us to build a FORTRAN program that uses the LAPACK librairies to handle the most important matrix operations. Once the program established, it was then possible for us to implement some of the different methods that are devised to handle the artifact of the back reflection at boundaries of the numerical box.

The implementation of the masking method is the easiest one as it is just a multiplication of the wave by the masking function. As for the complex absorbing potential (CAP), it is important to incorporate the potential in the hamiltonian matrix. These two suppression methods are non local and need an extra spatial interval in order to be efffective. This is the constraint of these two methods as this means the need for extra memory resources. The advantage of these methods is their effectiveness on a large energy range (around 70 for the masking method and 75 for the CAP). The performances of the two methods are quite similar however the CAP method is more systematic as we can evaluate the attenuation introduced by different potentials and thereby appreciate the way and the time needed for a complete cancellation of the wave amplitude.

We studied from another side the performances of a local method which is the absorbing boundary conditions (ABC). This method leads to a non tridiagonal hamiltonian matrix and thereby the propagator evaluation becomes slightly more complicated. The energy range on which this method is effective is very limited as it is related to the approximation needed for the linearization process. The major advantage of this method is the fact that it is local and does not need any extra spatial interval to be effective.

In summary it is important for us to know the specificities of the physical problem and performances of our machine and try to relate these facts with the performances of the different suppression methods in order to reach the best compromise.

Bibliography:

[1] E. Schrödinger, “The non relativistic équation of the de Broglie waves,” Ann. Physik79,361-376 (1926)
[2] J D Cresser .Chapter 6 The Schrodinger Wave Equation. 23rd May 2005 http://physics.mq.edu.au/~jcresser/Phys201/LectureNotes/SchrodingerEqn.pdf
[3] Richard Fitzpatrick 2010-07-20. Quantum Mechanics. http://farside.ph.utexas.edu/teaching/qmech/Quantum/node25.html
[4] Salah MENOUAR, these de doctorat (Université Ferhat Abbas de SETIF)
[5] Chen, Zuojing, "Efficient Modeling Techniques for Time-Dependent Quantum System with Applications to Carbon Nanotubes"(2010). Masters Theses 1911 - February 2014. https://scholarworks.umass.edu/theses/421
[6] J´uliaAlsinaOriol, Marc Basquens Muñoz, and Conrad Corbella Bagot.(Dated: May 24, 2016). Visualization of wave packets in Quantum Mechanics.Reflection and Transmission coefficientshttps://upcommons.upc.edu/bitstream/handle/2117/192493/pef2alsina-basquens-corbella.pdf?sequence=1&isAllowed=y.
[7] F. L. Dubeibe. International Journal of Modern Physics C · November 2010. Solving the Time-Dependent SCHRÖDINGER Equation with Absorbing Boundary Conditions and Source Terms in Mathematica 6.0.https://www.researchgate.net/publication/258397516.
[8] Yu, Youliang. Computationally Exploring Ultrafast Molecular Ionization. Manhattan, Kansas .2018.
[9] S. Yoshida, S. Watanabe ,C. O. Reinhold, J. Burgdorfer. Reflection-free propagation of wave packets. AUGUST 1999 The American Physical Society.
[10] Anna Nissen. Absorbing Boundary Techniques for the Time-Dependent Schrodinger ¨Equation .February 2010. Sweden. http://www.it.uu.se/
[11] C. W. McCurdy, C. K. Stroud, M. K. Wisinski. Solving the time dependent Schrodinger equation using complex-coordinate contours. Phys. Rev. A 43:5980{5990, 1991.
[12] N. Moiseyev, P. R. Certain, F. Weinhold. Resonance properties of complex-rotated hamiltonians. Molecular Physics 36:1613{1630, 1978.
[13] Hans-Dieter Meyer. NTRODUCTION TO MCTDH. July 2011 https://www2.chem.ucl.ac.uk/quantics/hdm_mctdh.pdf